

# Implementation of Digital Predistortion for RF/Microwave Transmitters

**Behbood Eskandariturk**

Electronics Systems Design and Innovation

Submission date: July 2022

Supervisor: Prof.Morten Olavsbråten



Fakultet for informasjons-  
teknologi og elektroteknikk

Institutt for elektroniske systemer

## **Abstract**

The emergence of extremely effective communication systems using higher order modulations has increased interest in linearization methods for nonlinear radio frequency power amplifiers. This is very important since the PA is a vital component of communication systems and because the nonlinearity produced by PAs causes spectrum regrowth and adjacent channel interferences, which degrade the system's performance. In this thesis, the linearization task is carried out using DPD, which has the Direct Learning Architecture, once the Behavioral model of the PA that needs to be linearized is established. Additionally, to obtain accurate results, different PA models are optimized using Least Square Estimation, which precisely compensates for the PA nonlinearity. The simulation results demonstrate that the DLA DPD is able to precisely improve the various Figures of Merits, including ACPR, NMSE, EVM, and STDR.

## Summary

Nowadays, higher modulation schemes are introduced in modern communication systems to support more customers, yet these new systems are quite sensitive to nonlinearity. PAs can be considered as the main source of nonlinearity in communication systems. For the PAs, there is a trade-off between linearity and efficiency, therefore if the system is to operate with high efficiency, it must operate in the nonlinear region. The constellation diagram is distorted and interference with the adjacent channels increases as the signal goes through the nonlinear PA, which are undesirable for new communication systems. To avoid this issue, the linearization techniques are used to acquire both linearity and efficiency. In this thesis, DPD is introduced as the linearization technique.

The DPD architecture can be divided into two main categories, namely the Indirect Learning Architecture and Direct Learning Architecture [1]. In the ILA, the normalized output signal is used as the input of the predistorter in such a way that the non-linear distortion of the PA is removed by introducing a predistorter block that has an inverse distortion characteristic of the PA. The cascade combination of the predistorter and the PA thus achieves a linear input/output relationship. On the other hand, the DLA is based on the identification of the PA Behavioral Model, whose reverse function is the DPD function to be calculated through several iterations and the implementation is required some parameters to be defined before performing the DPD.

The DLA consists of two main paths, namely forward path and the feedback [1]. In this thesis, to perform linearization, the DPD is used that utilizes the Direct Learning Architecture and the BMs that are used are made based on the Volterra series. The great advantage of using the BM is that they are describing the relationship between the input and output of the PA regardless of having knowledge about the PA circuitry. Four models have been used: the Saleh model, memoryless MP, GMP model and the MP model, which are then implemented in MATLAB Live Script and used to describe the behavior of five different PAs that have different tracking schemes (such as ET and PET for MAX PAE etc.). The results prove that the performance metrics such as ACPR, EVM, NMSE, STDR has improved significantly utilizing the DLA DPD.

# Preface

This thesis is written as the end of the 5-year master's degree in Electronics System Design and Innovation at the Norwegian university of science and technology (NTNU) in Trondheim. This project is lasted more time due to my employment and movement to Stavanger. One of my areas of interest is continuously learning new RF PAs techniques. One of the objectives of this thesis is to show that, despite some components not being designed with acceptable efficiency, some aspects of the communication system may be enhanced using software without modifying the hardware.

# Acknowledgements

I would first want to express my gratitude to Prof. Morten Olavsbråten of the NTNU Department of Electronic Systems, who helped me as my thesis adviser. He was a great help during the project, and I want to thank him for that. With tremendous care, he patiently went through every aspect of the thesis and supplied numerous helpful technical references. On this project, he consistently let me to work on my own, but when he thought I needed it, he directed me in the right direction.

I want to sincerely thank my mother for her steadfast encouragement and support throughout the years I spent studying in Norway.

# Contents

<b>1</b>	<b>Introduction</b>	<b>10</b>
1.1	Objectives . . . . .	10
1.2	Thesis outline . . . . .	11
<b>2</b>	<b>Theory</b>	<b>12</b>
2.1	Power Amplifiers . . . . .	12
2.1.1	Linear PA Classes . . . . .	12
2.1.2	Linear Gain . . . . .	13
2.1.3	Efficiency . . . . .	14
2.1.4	Gain Compression and AM/AM Characteristic . . . . .	14
2.1.5	Baseband Representation of PA . . . . .	15
2.2	Distortions . . . . .	16
2.2.1	Distortion effects on the Constellation Diagram . . . . .	16
2.2.2	Spectral Regrowth . . . . .	16
2.3	Performance Evaluation of PAs . . . . .	17
2.3.1	Error Vector Magnitude(EVM) . . . . .	17
2.3.2	Normalized Mean Square Error(NMSE) . . . . .	18
2.3.3	Signal to Total Distortion Ratio(STDTR) . . . . .	19
2.3.4	Adjacent Channel Power Ratio(ACPR) . . . . .	19
2.4	Memory Effects . . . . .	20
2.5	Linearization Techniques . . . . .	21
2.5.1	Analog Predistortion . . . . .	24
2.6	Digital Predistortion . . . . .	25
2.6.1	DPD Algorithm . . . . .	26
2.6.2	Digital Predistortion-Direct Learning Architecture(DLA) . . . . .	26
2.6.3	Power Alignment Issue . . . . .	28
2.7	Least Square Estimation to Model the Input-Output Relationship . . . . .	30
<b>3</b>	<b>Behavioral Modeling of Power Amplifiers</b>	<b>33</b>
3.1	Behavioral Models . . . . .	33
3.2	Preparation of Model . . . . .	34
3.3	Volterra Model . . . . .	34
3.4	Memoryless Nonlinear Model . . . . .	35
3.4.1	Saleh Model . . . . .	36
3.5	Nonlinear Models with Nonlinear Memory . . . . .	37
3.5.1	Generalized Memory Polynomial Model(GMP) . . . . .	37
3.5.2	Memory Polynomial Model(MP) . . . . .	38

<b>4</b>	<b>Implementation and Results</b>	<b>39</b>
4.1	Setup . . . . .	39
4.2	Results . . . . .	41
4.2.1	PA with Constant(static) Drain Voltage $V_d=28V$ . . . . .	41
4.2.2	PA Combined with MAX PAE Tracking Scheme . . . . .	46
4.2.3	PA Combined with Max PAE PET Tracking Scheme . . . . .	48
4.2.4	PA Optimized with ET for tracking Flat Gain =12dB . . . . .	50
4.2.5	PA Optimized with PET Tracking Flat Gain =12dB . . . . .	52
<b>5</b>	<b>Discussion</b>	<b>54</b>
<b>6</b>	<b>Conclusion</b>	<b>55</b>

# List of Figures

2.1	Loadline for the different PA classes . . . . .	13
2.2	Different input and output powers for a PA. . . . .	13
2.3	Loadline for the different PA classes. . . . .	14
2.4	The transfer function for a non-uniform memory polynomial model. . . . .	15
2.5	A simplified block diagram of transmitter/receiver [2] . . . . .	15
2.6	Nonlinear amplitude-phase model for complex baseband signals[2] . . . . .	16
2.7	Distortions of constellation . . . . .	16
2.8	The PA distortion has adverse effects on adjacent channels that is known as Spectral Regrowth. . . . .	17
2.9	EVM. . . . .	18
2.10	ACPR definition. . . . .	20
2.11	A simplified RF PA block diagram [2] . . . . .	20
2.12	Decomposition of Memory Effects for a RF PA[3] . . . . .	21
2.13	Basic block diagram of feedforward. . . . .	21
2.14	Block diagram of Feedback[4] . . . . .	22
2.15	Principle of Chirex (also called outphasing)[4] . . . . .	22
2.16	Block diagram of EER[5] . . . . .	23
2.17	Principle of ET[5] . . . . .	23
2.18	A brief summary of linearization techquies. . . . .	24
2.19	Block diagram of Predistortion . . . . .	25
2.20	A combination of a predistorter and PA . . . . .	25
2.21	Basic idea about combination a predistorter and PA . . . . .	26
2.22	Block diagram of the DLA DPD[1]. . . . .	27
2.23	Flow of steps for creating a PA BM follows by the DLA DPD. . . . .	28
2.24	The behavior of the device under test varies with the operating average power. . . . .	29
2.25	The gain change with respect to peak power [6] . . . . .	30
2.26	The PA Input and Output voltages. . . . .	31
2.27	The PA Input and Output voltages.. . . . .	31
2.28	The matrix representation of the equation 2.25 [7] . . . . .	32
3.1	Classification of memory effects for the Behavioral Modeling of non-linear RF PA .Unlike the AM/AM characteristic, which is always observed in any nonlinear device, phase distortion is only observed in dynamic devices such as PAs that contain memory[2] . . . . .	33
3.2	BM extraction procedure: key steps from measurements to model validation [6] . . . . .	34



3.3	Trade-off between complexity and performance of the different models such as block-oriented models(Hammerstein and Wiener) and MP that are the simplified version of the Volterra model. . . . .	35
3.4	The AM/AM and AM/PM characteristics of the PA. . . . .	36
3.5	The MATLAB curve fitting toolbox to find the Saleh's Coefficients. . . . .	37
4.1	The measurement setup[2] . . . . .	39
4.2	The PSD of output signals for PAs with different tracking schemes,without DLA DPD. . . . .	41
4.3	Results of simulation for the PA with static Vd=28V, without DLA DPD . . . . .	42
4.4	Results of simulation for a memoryless PA ,with DLA DPD. . . . .	45
4.5	Results of simulation for the PA with MAX PAE tracking, without DLA DPD . . . . .	46
4.6	Results of simulation for the PA with MAX PAE PET tracking, before DLA DPD . . . . .	48
4.7	Results of simulation for the flat gain PA with ET tracking, without DLA DPD . . . . .	50
4.8	Results of simulation for the flat gain PA with PET tracking, without DLA DPD . . . . .	52

# List of Tables

4.1	The instrument used for the measurements. . . . .	40
4.2	Input signal parameters . . . . .	40
4.3	Measured specifications of 5 different PAs at $f=2.0\text{GHz}$ with the different tracking schemes,without DPD. . . . .	41
4.4	Results of measurements for PA with constant drain voltage after applying the Memoryless DPD. . . . .	43
4.5	Results of measurements for PA with constant drain voltage after applying the MP DPD. . . . .	43
4.6	Results of measurements for PA with constant drain voltage after applying the GMP DPD. . . . .	44
4.7	Results of measurements for PA MAX PAE after applying the Memoryless DPD. . . . .	47
4.8	Results of measurements for PA MAX PAE after applying the MP DPD. . . . .	47
4.9	Results of measurements for PA MAX PAE after applying the GMP DPD. . . . .	47
4.10	Results of measurements for PA MAX PAE PET after applying the Memoryless DPD. . . . .	48
4.11	Results of measurements for PA MAX PAE PET after applying the MP DPD. . . . .	49
4.12	Results of measurements for PA MAX PAE PET after applying the GMP DPD. . . . .	49
4.13	Results of measurements for PA ET flat gain=12dB after applying the Memoryless DPD. . . . .	50
4.14	Results of measurements for PA ET flat gain=12dB after applying the MP DPD . . . . .	51
4.15	Results of measurements for PA ET flat gain=12dB after applying the GMP DPD . . . . .	51
4.16	Results of measurements for PA PET flat gain=12dB after applying the Memoryless DPD . . . . .	52
4.17	Results of measurements for PA PET flat gain=12dB after applying the MP DPD . . . . .	53
4.18	Results of measurements for PA PET flat gain=12dB after applying the GMP DPD . . . . .	53

# Abbreviations

**PAPR** Peak to Average Power Ratio  
**PAE** Power Added Efficiency  
**PA** Power Amplifier  
**QAM** Quadrature Amplitude Modulation  
**I/Q** In-Phase / Quadrature  
**ACPR** Adjacent Channel Power Ratio  
**EVM** Error Vector Magnitude  
**EER** Envelope Elimination and Restoration  
**ET** Envelope tracking  
**PET** Power Envelope tracking  
**DPD** Digital Predistortion  
**PD** Predistorter  
**MP** Memory Polynomial  
**GMP** Generalized Memory Polynomial  
**DUT** Device Under Test  
**AM/AM** Amplitude to Amplitude characteristic  
**AM/PM** Amplitude to Phase characteristic  
**PSD** Power Spectral Density  
**TWTA** Traveling-Wave Tube Amplifier  
**ARB** Arbitrary waveform generators  
**SA** Spectrum Analyzer  
**RF** Radio Frequency  
**MSE** Mean Squared Error  
**STDR** Signal to Total Distortion Ratio  
**RF** Radio frequency  
**NMSE** Normalized Mean Square Error  
**GaN** Gallium Nitride  
**HEMT** High-Electron-Mobility Transistor  
**FoM** Figure of Merit

# Chapter 1

## Introduction

The complexity of today's communication systems has increased the demand for Radio Frequency Power Amplifiers in terms of performance. In comparison to traditional constant envelope modulation systems, modern modulation techniques that enable higher data rates, longer battery life, etc are more complex and more prone to distortion because of non-linearities. As a result, there are higher demand for PAs' performance in terms of linearity. Linear RF PA is, however, inherently inefficient and will lose the majority of the DC power. Considerably worse, linear modulation schemes must be operated in the linear area of the PA, or in back-off, where efficiency is even lower. The PA is one of the major consumer of DC power, thus by improving the efficiency of the PA, the total system efficiency will be improved. Low efficiency in a system would reduce the battery life of portable devices[8]. DPD has demonstrated significant improvements in PA linearity with recent high-speed digital circuits by lowering FoM like the Adjacent Channel Power Ratio (ACPR) and Error Vector Magnitude (EVM), and has emerged as the most widely used technique for PA linearization [9].

There is no requirement for in-depth knowledge of the PA circuitry and its operation in DPD technique and the PA is considered as a black box[3]. The goal of this thesis is to increase the linearity of a PA using DPD technique, in which a predistorter stage is utilized in front of the PA to simulate the behavioral of the PA using the inverse of the PA behavioral model. This inverse model is then used at the predistorter stage to distort the input signal before exciting the PA.

### 1.1 Objectives

In this thesis, the main learning objectives are:

- To understand how PA nonlinearity can be generated.
- Assessing PA performance according to different criterion.
- Learning linearization techniques in detail, more specifically about DPD.
- Be familiar with the ILA, DLA, and DPD mathematical models.
- Application of the different BMs such as the Saleh model, MP and GMP and apply them to DLA DPD.

- Obtain experience with MP,GMP DPD software implementation in MATLAB Live Script, which enables simulations to run interactively.

## 1.2 Thesis outline

- **Chapter 2:** This chapter explains the nonlinearities of the PA. The parameters used to define the nonlinearity characteristics as well as its effects are introduced. Memory effects are discussed since it is expected that the distortions caused by memory effects will be linearized by the DPD. The linearization techniques are then briefly covered, but DPD is explained in great detail. The Indirect Learning Architecture explains briefly and for the Direct Learning Architecture, the theory and distortion are introduced. This chapter also covers the mathematical concept of Least Square Estimation that is essential method for optimization.
- **Chapter 3:** Behavioral Modeling of PAs will be explained in this chapter. also how the different models are made is discussed.
- **Chapter 4:** This chapter explains how to set up measurements using equipment. Here, the measured results are also presented and discussed.
- **Chapter 5:** The results from the measurements and how they compare to one another are briefly discussed in Chapter 5.
- **Chapter 6:** The thesis is finished in the conclusion chapter.

# Chapter 2

## Theory

### 2.1 Power Amplifiers

#### 2.1.1 Linear PA Classes

A PA's linearity is determined by its conduction angle, which is the portion of the signal cycle when current flows through the load. Figure 2.1 illustrates the different load lines and operating points for different classes of linear PAs. Using the conduction angle, PAs can be classified as A, B, AB, and C, which are briefly explained as follow:

- **Class A:** In class A amplifiers, current flows constantly through the load during the entire period of the input signal, resulting in a conduction angle of  $\alpha = 2\pi$ . Although the performance of a class A amplifier is highly linear, its power efficiency is the poorest among the four classes of PAs by  $\eta = 50\%$  [2], [10].
- **Class AB:** Amplifiers in class AB have a conduction angle between  $\pi < \alpha < 2\pi$ , and the bias voltage is between the threshold voltage and the Class A bias [10].
- **Class B:** For class B amplifiers,  $\alpha = \pi$  and the bias voltage equals the threshold voltage. There is no current half of the signal duration, when the input voltage is under the threshold voltage. The maximum theoretical drain efficiency for a class-B PA is  $\eta = 78.5\%$ . [10].
- **Class C:** For an amplifier in class C, the conduction angle is  $\alpha < \pi$  and the bias voltage is smaller than the threshold voltage. The transistor usually doesn't conduct and has a zero output current most of the time. The maximum theoretical efficiency equals  $\eta = 100\%$ . [10] [2].

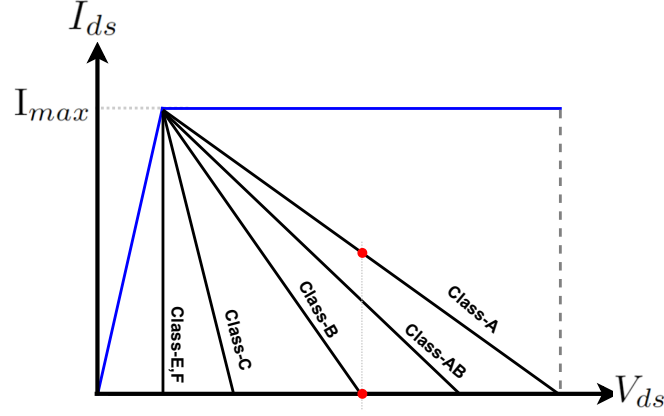


Figure 2.1: Loadline for the different PA classes [2]

### 2.1.2 Linear Gain

The gain of a PA is defined by the ratio between the output power and the input power.

$$G = \frac{P_{out}}{P_{in}} \quad (2.1)$$

A PA is an efficient converter capable of converting DC power to RF power. It transforms the power provided by the power supply into a high output power and adds it to the RF input signal[1]. Some of this DC power is, however, not converted to RF but instead will be dissipated thermally.

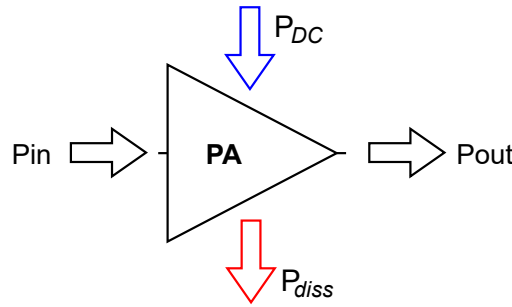


Figure 2.2: Different input and output powers for a PA.[2]

From figure 2.2 ,the relationship between the input powers and the output power can be written as :

$$P_{out} + P_{diss} = P_{in} + P_{DC} \rightarrow P_{out} = P_{in} + P_{DC} - P_{diss} \quad (2.2)$$

Putting Equation 2.2 into Equation 2.1 yields [1]:

$$G = \frac{P_{in} + P_{DC} - P_{diss}}{P_{in}} \rightarrow G = 1 + \frac{P_{DC} - P_{diss}}{P_{in}} \quad (2.3)$$

From equation 2.3, it can be noticed that the gain of a PA cannot be constant when the input power increases that means the power supply voltage is a fixed value, but the input power could change.

### 2.1.3 Efficiency

One way to evaluating the efficiency in a PA is by measuring the drain efficiency (or the power supply efficiency  $\eta_{DC}$ ), which is a ratio between the average output power delivered to the load by the PA and average DC power added to the transistor drain [11].

$$\eta_{DC} = \frac{P_{out}}{P_{DC}} \quad (2.4)$$

However, This measurement does not consider the input power to the PA, therefore it is a simple way of evaluating the power efficiency. Power Added Efficiency (PAE) is a better measure that includes the effect of input power for evaluating the efficiency [11].

$$PAE = \frac{P_{out} - P_{in}}{P_{DC}} = \eta \left(1 - \frac{1}{G}\right) \quad [\%] \quad (2.5)$$

### 2.1.4 Gain Compression and AM/AM Characteristic

The figure 2.3 shows a typical power amplification characteristic and gain response for an RF PA operating at the fundamental frequency.

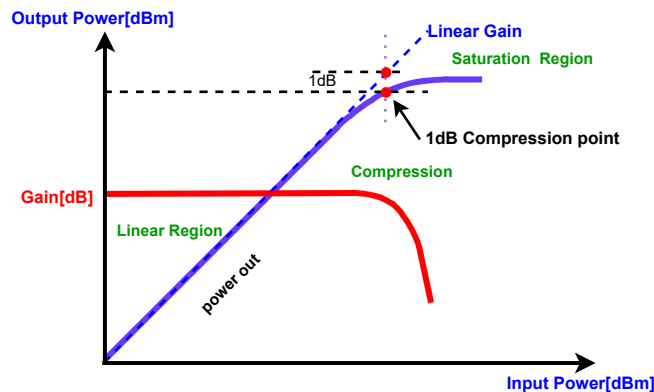


Figure 2.3: Power output and gain compression characteristics of a PA.

At low powers, the linear region exists, but since it is a small signal region, it is unlikely to be linear for any practical RF PA. With increasing power, the output power and gain deviate considerably from the linear relationship at small signals. In addition to the linear region, there is the compression region of operation, where, at sufficiently high input drive, the PA cannot produce any more power at which the PA is very nonlinear. The saturated region is characterised by the PA exhibiting very nonlinear behavior [7]. This type of compression is also known as AM-to-AM conversion, in which the output signal's amplitude varies when the input signal's amplitude changes. Often, this strong nonlinearity is referred to as the 1-dB gain compression point at which the output power is one decibel below the small signal [11].



Figure 2.4 illustrates that there is an inverse relationship between linearity and efficiency of PAs which means that the most efficient operation is obtained in the nonlinear region.

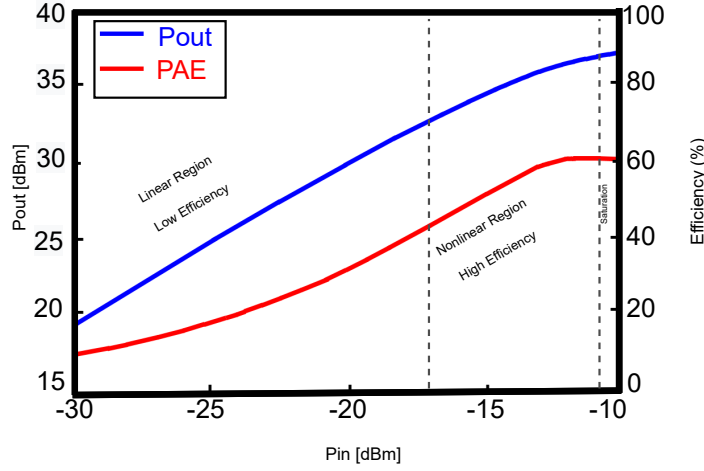


Figure 2.4: Output power and Efficiency versus Input power of a PA of class AB.

### 2.1.5 Baseband Representation of PA

For the models to represent a PA model, a baseband discrete signal is used, which can be represented in polar or cartesian coordinates as:

$$x[n] = \underbrace{I[n] + \mathbf{j}Q[n]}_{\text{cartesian}} = \underbrace{A[n] e^{\mathbf{j}\phi[n]}}_{\text{polar}} \quad (2.6)$$

where  $A[n]$ ,  $\phi[n]$  denote the amplitude and phase of the signal  $x[n]$ . Figure 2.5 shows a simplified block diagram of a communication system, in which the input signal  $x[n]$  and the output signal  $y[n]$  are complex-valued signals [3]:

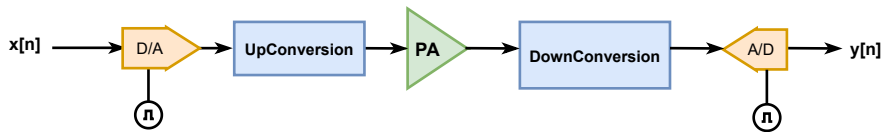


Figure 2.5: A simplified block diagram of transmitter/receiver [2]

The relationship between the input signal and the output signal of the PA can be expressed as:

$$y[n] = \mathbf{AMAM}(|x[n]|) e^{j(\phi[n] + \mathbf{AMPM}(|x[n]|))} \quad (2.7)$$

where **AMAM** characteristic, as explained in section 2.1.4, describes the gain compression of a PA compared to different input power levels with a fixed input frequency, while the **AMPM** characteristic explains how the PA output differs from the original input signal ( $x[n]$ ) based on the input power level. Therefore, AM/AM characteristic refers to the relationship between the output amplitude and the input

amplitude of a nonlinear system, while AM/PM characteristic, that is shown in figure 2.6, corresponds to the relationship between the phase change of the input and output signals, and the amplitude of the input signal.

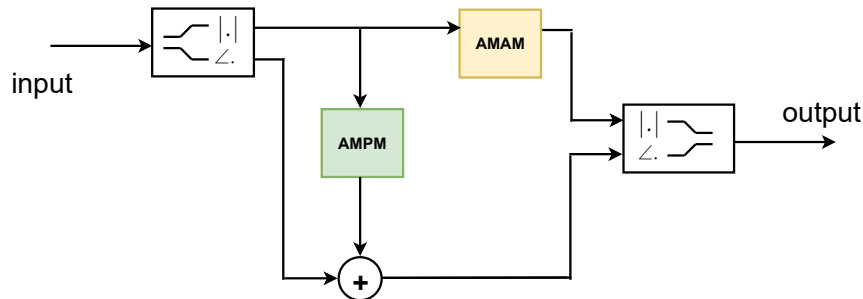
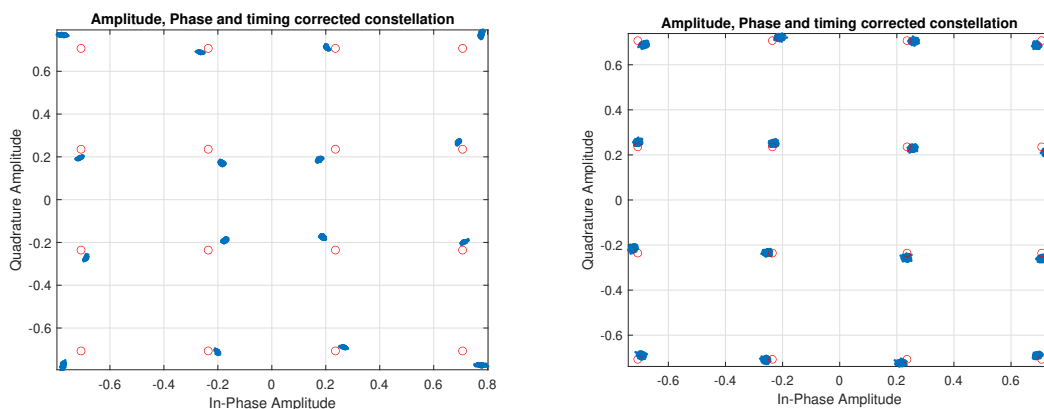


Figure 2.6: Nonlinear amplitude-phase model for complex baseband signals[2]

## 2.2 Distortions

### 2.2.1 Distortion effects on the Constellation Diagram

The effect of I/Q imbalance and skewness is illustrated in Figure 2.7. In the figure, it can be seen that the constellation points are no longer in the ideal positions and the I and Q branches are not orthogonal. The distance between constellation points has also changed, which will result in a decrease in the system's performance[4].



(a) The constellation is negatively affected by I/Q imbalance and rotation. The red dots represent the ideal 16-QAM, and the blue dots represent the output distortion.

(b) The negative effects of PA distortion on the constellation of the input signal. Red dots indicate a 16-QAM ideal input, while blue clouds indicate distortion created at the output signal of the PA.

Figure 2.7: Distortions of constellation

### 2.2.2 Spectral Regrowth

The distortions produced by the transmitter also affect the frequency response of a communication system, leading to a phenomenon called as spectrum regrowth. This

is equivalent to the spectral leaking of power into adjacent frequency spectrum channels. Since linear components do not cause spectrum regrowth, spectral regrowth is a result of the transmitter's nonlinearity[3]. The effects of a PA distortion in the frequency domain are depicted in Figure 2.8.

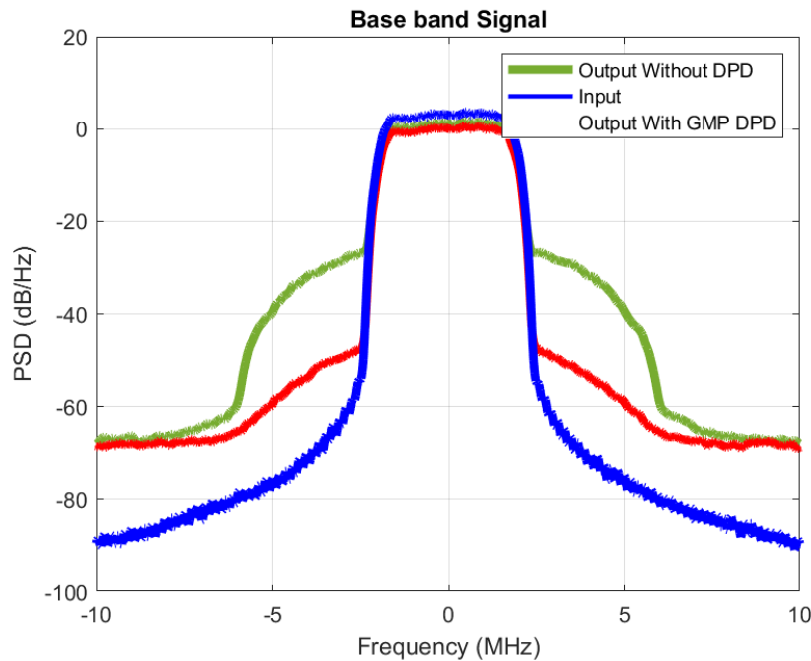


Figure 2.8: The PA distortion has adverse effects on adjacent channels that is known as Spectral Regrowth.

## 2.3 Performance Evaluation of PAs

This section contains the most common Figures Of Merits to evaluate the performance of DPD. It is worthwhile to mention that the NMSE and EVM accesses the DPS performances in time domain, While the ACPR evaluates the DPD modeling performance in the frequency domain.

### 2.3.1 Error Vector Magnitude(EVM)

Figure 2.9 illustrate a common method for measuring in-band distortions that is called EVM, which measures the magnitude of the error vector between the ideal and measured signal vectors in the I/Q constellation diagram.

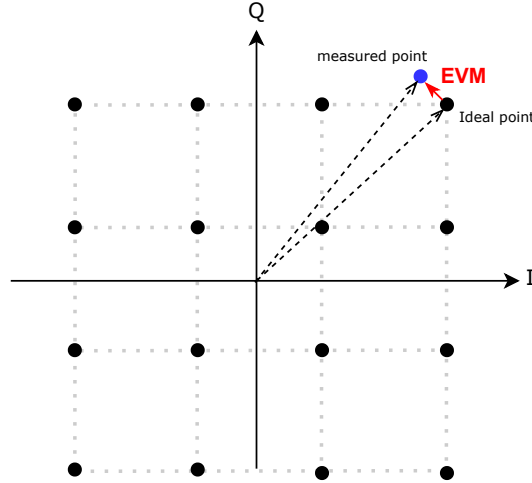


Figure 2.9: EVM.

The EVM can be calculated as [12]:

$$EVM = \frac{\text{mean}(|x_{ideal} - x_{meas}|)}{\text{mean}(|x_{ideal}|)} \times 100 \quad [\%] \quad (2.8)$$

where the  $x_{ideal}$  and  $x_{meas}$  are the ideal(reference) and measured signal vectors ,respectively.

### 2.3.2 Normalized Mean Square Error(NMSE)

The ultimate objective of wireless transmitters is to minimize the difference between the system's output signal and the desired output signal that would have been delivered to the antenna. This difference can be expressed as:

$$e[n] = y_{measured}[n] - y_{desired}[n] \quad (2.9)$$

where  $y_{measured}[n]$  is the sampled measured output of the system,  $y_{desired}[n]$  is the sampled intended output that should be sent to the antenna, and  $e[n]$  is the error signal. In terms of accuracy, the simplest metric is to use the expression 2.9 to determine Mean Squared Error (MSE) for the transmitter [4]. The MSE is calculated as follows:

$$MSE = \sum_n |y_{measured}[n] - y_{desired}[n]|^2 \quad (2.10)$$

The Normalized MSE(NMSE) used in this thesis can be defined as [13]:

$$NMSE = 10 \times \log_{10} \left( \frac{\sum_{i=1}^M |y_i - \hat{y}_i|^2}{\sum_{i=1}^M |y_i|^2} \right) \quad [dB] \quad (2.11)$$

where the modeled PA output is  $\hat{y}_i = \hat{y}(i)$  and the measured PA output is  $y_i = y(i)$ . It should be noted that the NMSE decreases as the model order increases which leads to the higher accuracy for the model; however, the model's instability increases as the nonlinear order increases. Because of this, when a model must be chosen, a compromise must be made between model accuracy and model stability[13]. A lower NMSE indicates that the model can more accurately capture the nonlinear behavior of the PA and is predicted to perform better during predistortion linearization[12].

### 2.3.3 Signal to Total Distortion Ratio(STDR)

Using STDR has the benefit of accounting for any out-of-band non-linearities and allowing the performance evaluation to be made independent of the bandwidth of neighboring channels[14]. STDR evaluates the nonlinear distortion that appears both in-band and out-of band of the signal, It can be used for evaluating the overall linearity of a system. Optimizing the PA for maximum STDR leads to maximize the ratio of the linear over nonlinear power of the output signal. As is explained in[14] ,the average input power can be expressed as  $I_a$  and calculated as:

$$I_a = \frac{1}{T} \int_0^T |a(t)|^2 dt \quad (2.12)$$

where  $a(t)$  is the input signal.Similarly, $I_b$  is the average total output power and expressed as:

$$I_b = \frac{1}{T} \int_0^T |b(t)|^2 dt \quad (2.13)$$

where ,  $b(t)$  is the output signal. $I_x$  is twice the power of the baseband signal, and expressed as [14]:

$$I_x = \frac{1}{T} \int_0^T b(t)^* a(t) dt \quad (2.14)$$

As described in [14] STDR can be described as:

$$STDR = 10 \log_{10} \left( \frac{I_a I_b}{I_a I_b - |I_x|^2} \right) \quad [dB] \quad (2.15)$$

### 2.3.4 Adjacent Channel Power Ratio(ACPR)

Adjacent-Channel Interference (ACI) is a spectral broadening (spectral regrowth) in communication systems caused by nonlinear amplification [13].Establishing a lower limit on the power in the main channel to the amount of power induced in the adjacent channel is still necessary.The adjacent channel power ratio (ACPR) is used to determine how much power is leaked from the transmitter into adjacent channels in applications where the out-of-band is crucial. ACPR is defined in terms of the PSD of the output of a nonlinearity as:

$$ACPR = 10 \log_{10} \left( \frac{\int_{f_1}^{f_2} Y(f) df}{\int_{f_3}^{f_4} Y(f) df} \right) \quad [dB] \quad (2.16)$$

Where the higher neighboring channel's limits are at frequencies  $f_3$  and  $f_4$ , whereas the main channel's limits are at  $f_1$  and  $f_2$  , and  $Y(f)$  is the PSD of the PA output. The definition of ACPR and the associated frequency restrictions are made clear in Figure 2.10 [13].The main channel is used for the integration in the numerator and neighboring channels are used for the integration in the denominator. This metric can accurately depict the degree of distortion produced in a communication system's adjacent channels, which is vital in many applications.

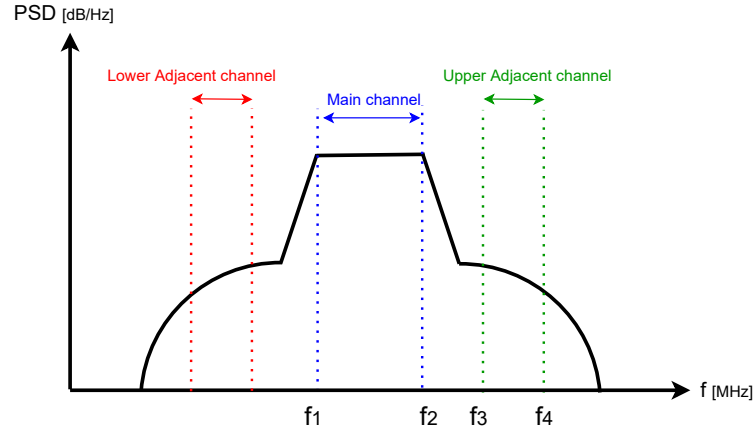


Figure 2.10: ACPR definition.

## 2.4 Memory Effects

Both PAs and TWTAs have commonly been described using cascades of linear filters combined with a memoryless nonlinearity, or what are known as two-box models. This is an obvious result of linear memory effects at the input and output of the device, which can be physically related to the PA's input and output tuned networks. This type of linear memory referred to the short-term memory effects that are in range of  $ns$ . In addition to these linear memory effects, there are additional dynamic effects that only manifest when nonlinear regimes are present and called long-term memory effects, which are typically related to the bias circuits, thermal interactions, and active-device low-frequency dispersion and they are in the range of  $\mu s$  to  $ms$  [3]. Figure 2.11 shows these memory effects in RF PA circuits.

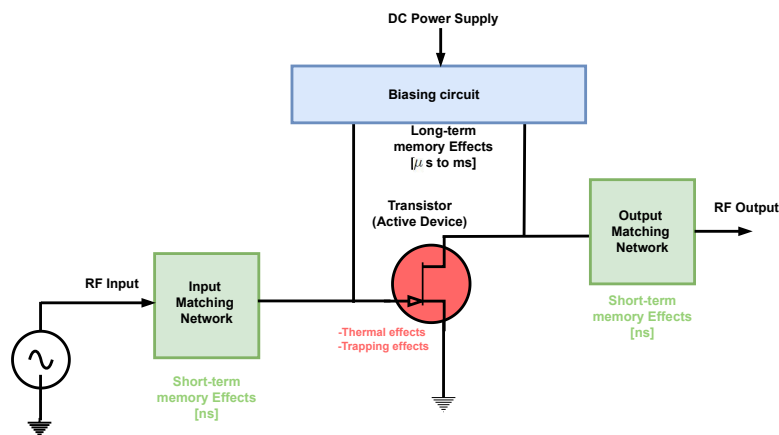


Figure 2.11: A simplified RF PA block diagram [2]

Furthermore, these nonlinear dynamics are described by the dynamic interaction of two or more nonlinearities through a dynamic network and cannot be modeled by

any noninteracting linear filter or memoryless nonlinearity box models. As is shown in figure 2.12, memoryless nonlinearity and a filter in a feedback path can be used to describe such effects. The filters  $H(w)$  and  $O(w)$  represent linear memory effects because of input and output matching networks, and  $F(w)$  represents non-linear memory due to thermal hysteresis, trapping and bias circuit [3].

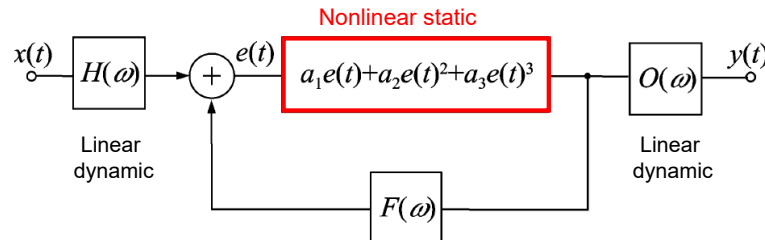


Figure 2.12: Decomposition of Memory Effects for a RF PA[3]

## 2.5 Linearization Techniques

Different linearization techniques are available to minimize distortions resulting from nonlinearity and memory effects. In this section, some typical techniques are briefly explained. In general, the three types of analog techniques are feedback, feedforward and predistortion techniques. Figure 2.13 illustrates an analog feedforward linearization, a method for reducing distortion that involves adding a phase-reversed version of the error signal to the PA's output, which compares the output of the main amplifier, A1, to a delayed version of the input signal. The difference between input signal and error from A1 are then amplified in A2 and then added to the delayed output signal in such a way that all errors (or distortions) at the output signal are canceled [10].

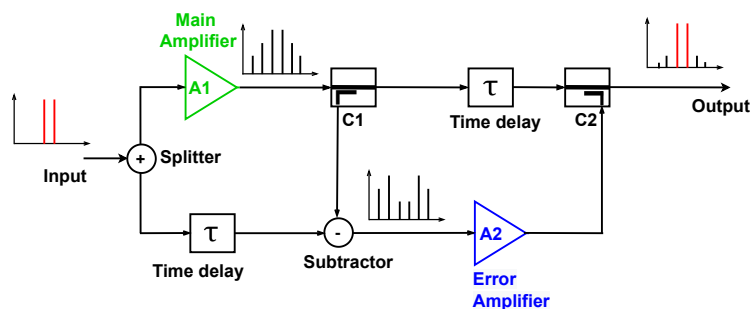


Figure 2.13: Basic block diagram of feedforward.

Figure 2.14 shows a linearization feedback technique. In analog feedback a portion of the output signal is taken using a feedback loop and subtractor (comparator) then calculates the error of the signal from the input signal and feedback signal. This error signal is injected to the input of the PA with a proper gain to cancel distortion [5].

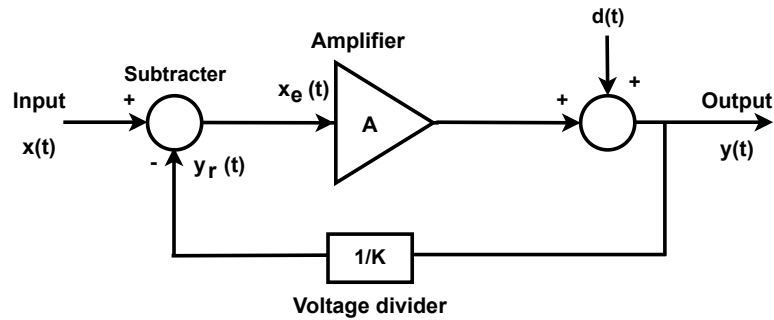


Figure 2.14: Block diagram of Feedback[4]

These methods often have the advantage of handling large input signal bandwidths, but they are typically expensive to use and frequency-sensitive. Another analog technique is called Chirex(outphasing) which originally was suggested as a technique to improve power efficiency , but can be seen as a linearization method .Chirex consists of two highl-efficient PA(class C,E,F,etc.) and acts by creating two constant envelop signals in such a way that the vector sum of PAs becomes equal to the input signal[10].The output of PAs are then combined in a Chirex coupler that provides outphasing.Figure 2.15 shows a simple diagram of the Chirex technique.

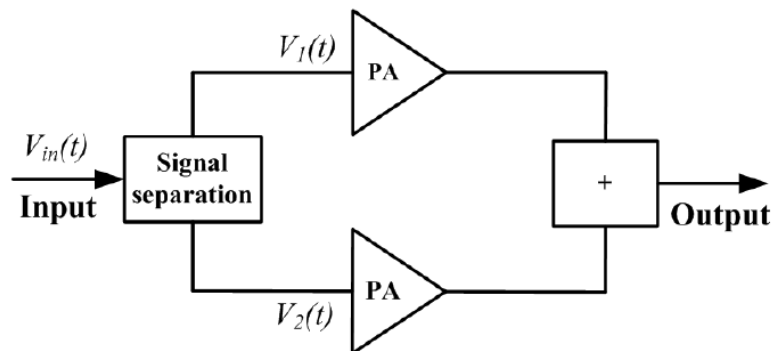


Figure 2.15: Principle of Chirex (also called outphasing)[4]

Envelope elimination and restoration(EER) is another linearization methode in which the envelope is removed from the input signal.The remaining phase og signalis then sent in to the RF PA,which operates in class C,E or F[10].The envelope is switched on again by modulating the drain voltage of the PA.Figure 2.16 illustrate EER technique.



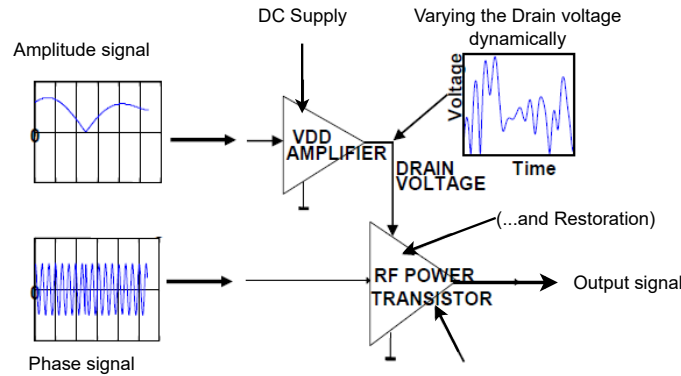


Figure 2.16: Block diagram of EER[5]

In Envelope tracking (ET) technique, the signal is amplified through a standard PA of class A, AB, B, or F. In order to improve the efficiency of the PA, an envelope is used to reduce the drain voltage (which is called the 'tracker' envelope) of RF PA with constant gain when the envelope is small [10]. ET allows the PA to operate near the saturation for all envelope levels [10]. Figure 2.17 shows a block diagram of ET technique.

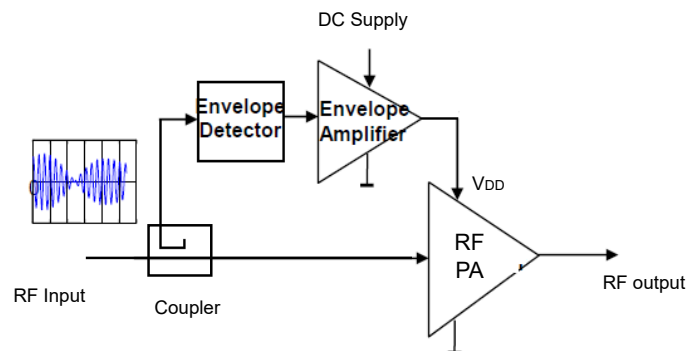


Figure 2.17: Principle of ET[5]

Power Envelope Tracking (PET) is another technique that was introduced in [15]. Using the formula  $A = I^2 + Q^2$  and the power of the envelope, power envelope tracking (PET) produces the drain tracking function. When compared to ET, this drastically reduces the tracking bandwidth at the cost of some efficiency. The order of the PET can be increased, meaning that when a second-order PET is compared to a pure PET, the signal bandwidth will be doubled, but the drain efficiency is more comparable to that of ET [15].

Envelope elimination and restoration(EER)envelope tracking (ET) have also been viewed as techniques for improving the linearization/power efficiency trade-off.Figure 2.18 illustrates a breif summary of the linearization techniques that explained in this section.

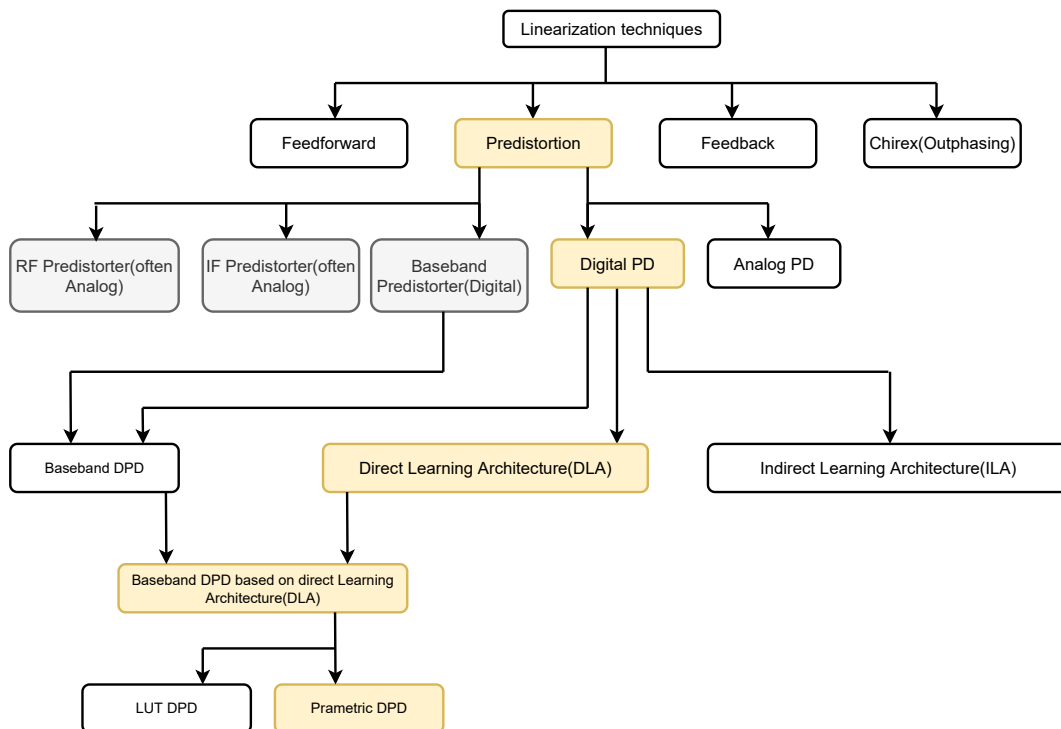


Figure 2.18: A brief summary of linearization techquies.

### 2.5.1 Analog Predistortion

Another important method for linearizing PAs is predistortion (PD). Figure 2.19 shows how a predistortion circuit is put before the PA. In order to create a new pre-distorted input for the nonlinear PA, this circuit inverses the nonlinear characteristic of the PA meaning that it creates signal components with proportionally inversed amplitude and opposite phase compared to the distortion products[61]. resulting in a system that has a linearized characteristic.

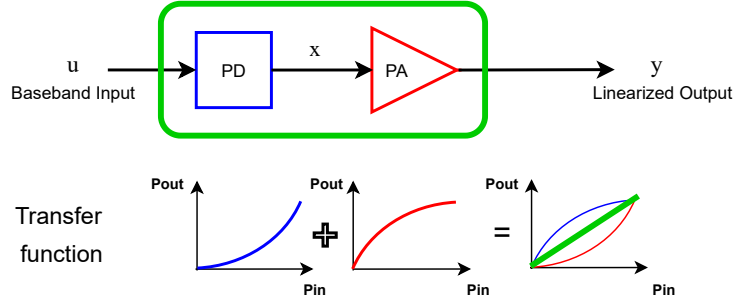


Figure 2.19: Block diagram of Predistortion

## 2.6 Digital Predistortion

Figure 2.20 shows the block diagram for the digital predistortion. Such technique is referred to Indirect Learning Architecture (ILA) [1]. The predistorter and nonlinear PA are combined to provide the ideal small signal gain,  $G$ .

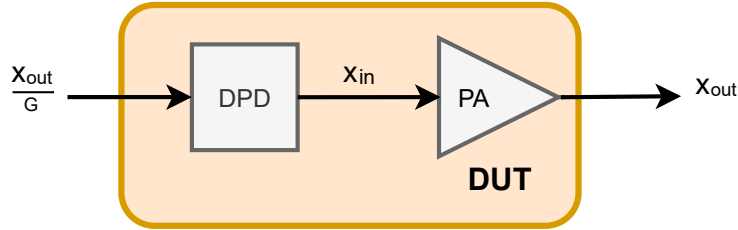


Figure 2.20: A combination of a predistorter and PA

Consequently, it can be said that the predistorter's input is normalized with  $G$  as :

$$x_{inDPD}(n) = \frac{x_{out}(n)}{G} \quad (2.17)$$

where  $x_{out}$  is the output of the PA and  $G$  denotes small signal gain. Equation 2.18 gives the output following the predistorter as [6]:

$$f_{DPD}\left(\frac{x_{out}(n)}{G}\right) = x_{in}(n) \quad (2.18)$$

The predistorter output, is input into the PA according to the equation below:

$$f_{DUT}(x_{in}(n)) = x_{out}(n) \rightarrow f_{DUT}\left(f_{DPD}\left(\frac{x_{out}(n)}{G}\right)\right) = x_{out}(n) \quad (2.19)$$

Here, the predistorter function,  $f_{DPD}$ , is equal to the BM of the reverse function of the PA generated by swapping the input and output signals of the PA with the proper small signal gain normalization. The input output relationship is linear following the

predistorter and PA cascade system, and the power no longer saturates at the level as before. DPD is the major digital technique for correcting distortion caused by the PA nonlinearity [6]. This method involves passing the signal via a digital version of the PA's inverse function. The system's total response will be linear if the inverse function of the PA is created precisely. The DPD technique has proven to lower the complexity, computation size, and cost for distortion mitigation compared to other linearization methods[9] since it makes use of a digital signal processing chain that can be implemented in MATLAB. However, it is crucial to create accurate models of the PA first in order to calculate the inverse of the PA characteristics.

### 2.6.1 DPD Algorithm

Figure 2.21 illustrates the basic idea of DPD. The red line shows the PA's nonlinear behavior, while the orange line shows the desired linear response.

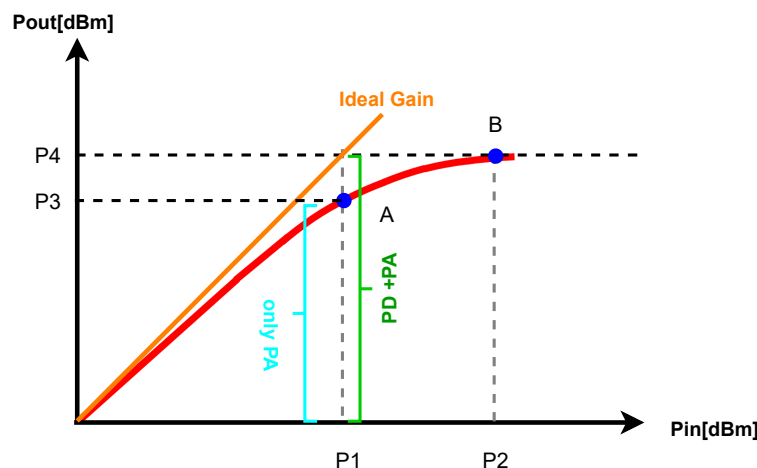


Figure 2.21: Basic idea about combination a predistorter and PA

Consider the point A as representing the input signal and assume that  $P_1$  is the average input power. Then  $P_3$  represents the corresponding average output power. The linear output power for  $P_1$  should be  $P_4$ , which corresponds to the average input power  $P_2$ . This means that the desired predistorted signal should be at point B, and the new input signal of the PA should have average input power  $P_2$ . Due to the nonlinearity, as the point A moves on the red curve to the right, the ratio  $P_2/P_1$ , which represents the input amplitude ratio of the point B to the point A, increases [4]. Keep in mind that the DPD won't be able to completely correct the nonlinearity if point B is beyond the saturation point.

### 2.6.2 Digital Predistortion-Direct Learning Architecture(DLA)

As it can be seen from figure 2.22, DLA consists of two different parts namely the forward path and the feedback path. The forward path produces the inverse of the PA behavioral model is used directly to construct the DPD, while the feedback path utilizes iterative optimization procedures for the coefficients of the DPD to minimize the error.

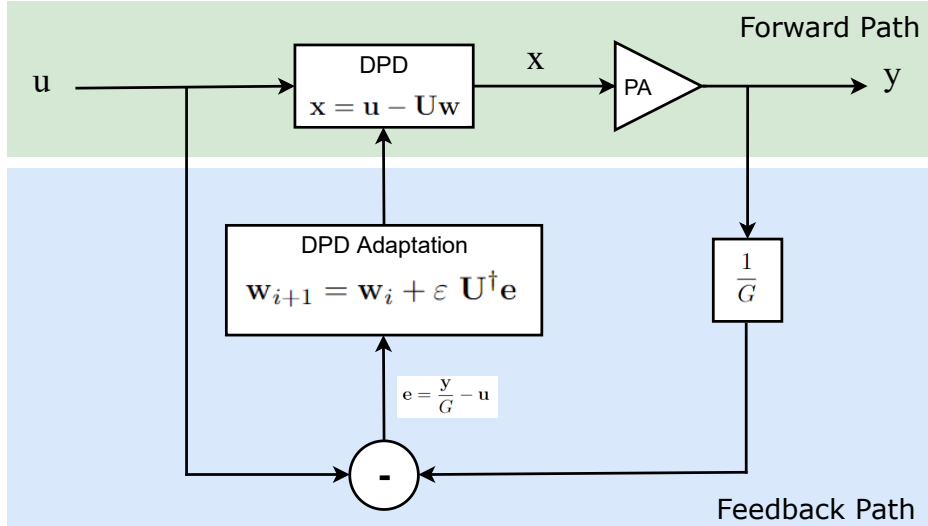


Figure 2.22: Block diagram of the DLA DPD[1].

The gain block,  $\frac{1}{G_0}$ , normalizes the amplitude of the output signal, and then this normalized output is subtracted from the input signal in order to calculate the amount of error,  $\mathbf{e}$ , that is written as:

$$\mathbf{e} = N\left[\frac{\mathbf{y}}{G_0}\right] - \mathbf{u} \quad (2.20)$$

There are different ways to calculate  $\mathbf{e}$ , but the most straightforward is to use the inverse of the Volterra-based series model and then applying it to the error by multiplying it with the step size which is a value between  $0 < \epsilon < 1$  to speed up the convergence. In this way, it is possible to calculate the predistorter coefficients  $\mathbf{w}_{i+1}$  adaptively until the error is decreasing [1]. This adaptation can be expressed as :

$$\mathbf{w}_{i+1} = \mathbf{w}_i + \epsilon \mathbf{U}^\dagger \mathbf{e} \quad (2.21)$$

where the  $\mathbf{U}^\dagger$  is the pseudo-inverse of the model which is calculated as:

$$\mathbf{U}^\dagger = (\mathbf{U}^H \mathbf{U}^H)^{-1} \mathbf{U}^H \quad (2.22)$$

Before sending the signal to the PA, the DPD will add the distorted signal,  $\mathbf{x}$ . Here,  $\mathbf{u}$  is the input vector, and  $\mathbf{U}$  is the measurement matrix made up of the *Regressors*, which are dependent on the input of the DPD. The coefficient vector,  $\mathbf{w}$ , contains the coefficients of the predistorter. A *Regressor* is a function of the input that normally consists of multiplications of the input and conjugate versions of it. (Both can be delayed). Then, the predistorter is updated through each iteration, as seen in figure 2.22. This predistorted signal can be expressed as:

$$\mathbf{x} = \mathbf{u} - \mathbf{U}\mathbf{w} \quad (2.23)$$

Thus, the predistorted signal is produced by subtracting the input signal,  $\mathbf{u}$ , from the product of the measurement matrix times the coefficient vector ( $\mathbf{U}\mathbf{w}$ ).

As shown in figure 2.23, there are pre-set parameters that have to be set before running the DPD DLA, meaning that modifying them leads to another new results and they are treated as the constant values in each iteration.

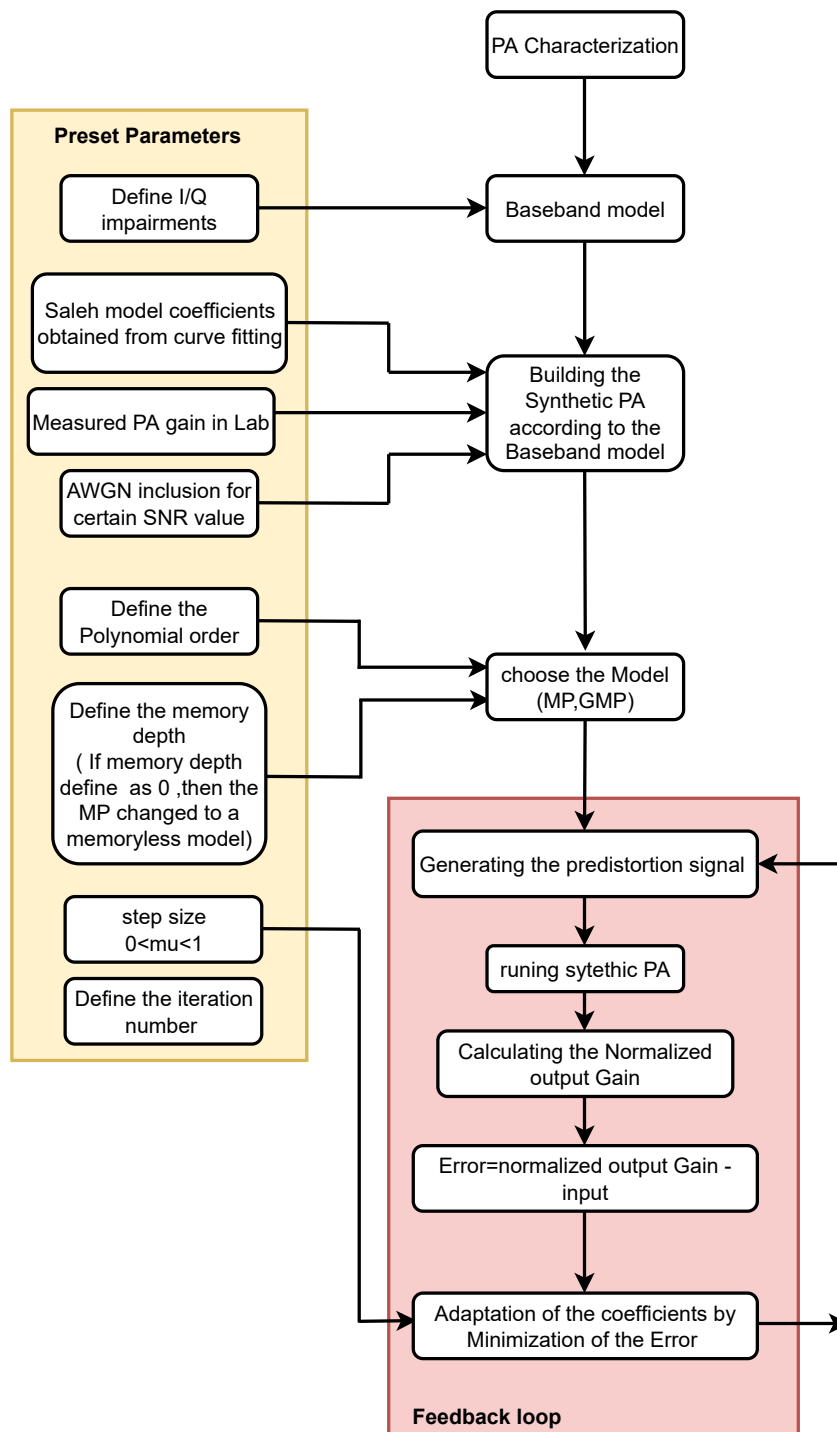


Figure 2.23: Flow of steps for creating a PA BM follows by the DLA DPD.

### 2.6.3 Power Alignment Issue

Essentially, the DPD technique entails applying a complementary nonlinear function upstream of the PA, allowing the predistorter and PA to act like a linear amplification system. Therefore, the linearized PA's performance is greatly impacted by

the nonlinear predistortion function implemented and its ability to compensate for the nonlinearity of the PA. The PD algorithm uses the output signal that has been normalized by the small signal gain. This step is performed to ensure that there is a power alignment between the predistorter and the PA. In a predistortion scheme, the PA input signal differs depending on whether it passes through the PA directly or after it passes through the predistorter in the forward path branch. Therefore, the responses of the PA can differ depending on the average power input [9]. As can be seen in figure 2.24, the PA's response is not so much impacted by the peak-to-average signal, but by the operating power. That is why the power alignment is done in order to avoid this. As a result of power alignment, the PA input power is kept stable, so there is no difference between its responses during characterization and linearization.

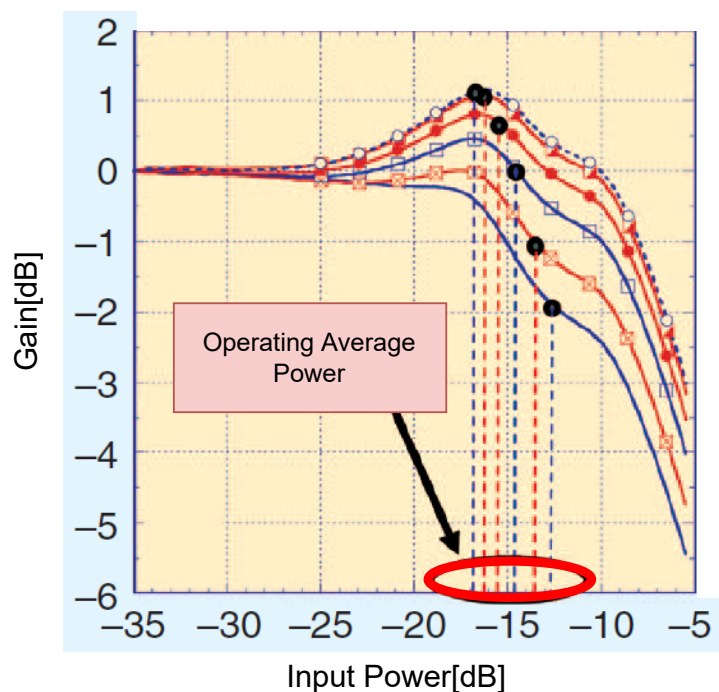


Figure 2.24: The behavior of the device under test varies with the operating average power.

In the case of a weakly nonlinear PA (such as class AB), small gain normalization ensures alignment of power between the PA and the PD. In contrast, for highly nonlinear PA (that biased in deep class AB or class B), if the PA output is normalized (explained in section 2.6.2) with a small signal gain (similar to weakly nonlinear PA), the average power variation is inevitable. Depending on the shape of the PA nonlinearity and the average power of the input, the gain normalization of highly nonlinear PAs varies [9].

The PA with high nonlinearities is not normalized properly, which means that the input average power of the PA varies after passing through the PD, resulting in variation in the PA's response. When the PA's response changes, the parameters found for the distortion become useless because they are estimated using the previous PA's

response, which causes the estimation of parameters to be repeated [6]. To tackle this issue, instead of going back to the PA characterization step due to insufficient linearization caused by power misalignment, the proper normalization gain can be applied in the DPD algorithm step as shown in figure 2.25.

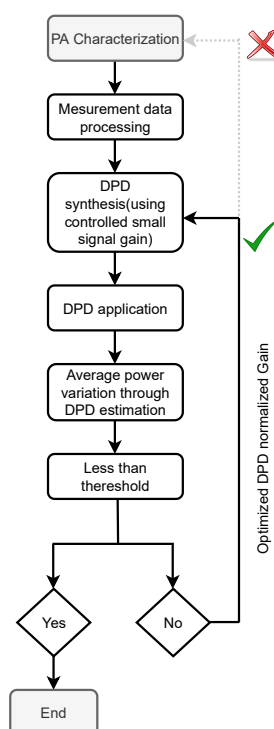


Figure 2.25: The gain change with respect to peak power [6]

## 2.7 Least Square Estimation to Model the Input-Output Relationship

When performing the DPD, it is crucial to solve a series of linear equations in order to get the optimal DPD coefficients. The least square estimation can be used for this. Figure 2.26 shows the IV characteristics and load line indicating that at large signal amplitudes, the voltage enters the knee region, and the current must fall correspondingly.



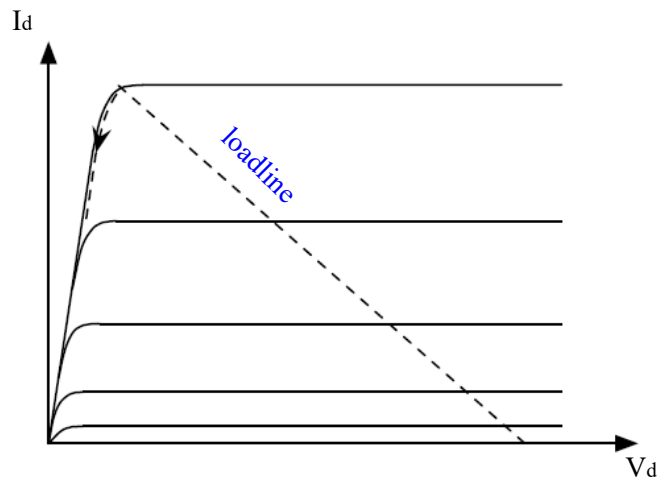


Figure 2.26: The PA Input and Output voltages.

The output power is related to the input power by what at first sight appears to be a very simple function. Some elementary curve-fitting should allow to model this relationship. Before diving into the mathematical expressions, let's review the goal. The main objective is to find a smooth function that approximates the measured input power–output power data in such a way that it fits the data with the minimum of error. This function is the model that should not expect the model to go through all of the data points exactly. The input-output curve is clearly nonlinear, so depending on the nonlinearity curve, the selection of the nonlinearity function and its degree is arbitrary and can be polynomials, exponential, etc. to make it possible to explain the physical outcomes of this input-output relationship. This choice makes it possible to write the model as a series of nonlinear basis functions that are linear in the parameters of the model. Linear-in-parameters means that the nonlinearity is captured by the basis functions, and the model fit is determined by the coefficients, enabling linear mathematical techniques to be applied to solving this problem [7].

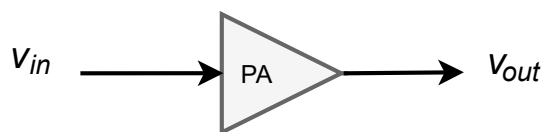


Figure 2.27: The PA Input and Output voltages..

According to figure 3.1, the polynomial expression in terms of the input and output voltage of the PA can be written as :

$$v_{out}(t) = a_1 v_{in}(t) + a_2 v_{in}^2(t) + \dots + a_N v_{in}^N(t) = \sum_{n=1}^N a_n v_{in}^n(t) \quad (2.24)$$

where the parameters that form the model are represented by the values of the coefficients as  $a_n$  and  $N$  is the degree of the polynomial. The linear gain is represented by the parameter  $a_1$  [7].

In the matrix representation , the expression  $\mathbf{x}$  can be written as :

$$v_{in}\mathbf{A} = \mathbf{v}_{out} \quad (2.25)$$

or by expansion,it can be written as :

$$\begin{bmatrix} v_{in}(t_1) & v_{in}^2(t_1) & \cdots & v_{in}^N(t_1) \\ v_{in}(t_2) & v_{in}^2(t_2) & \cdots & v_{in}^N(t_2) \\ \vdots & \vdots & \ddots & \vdots \\ v_{in}(t_T) & v_{in}^2(t_T) & \cdots & v_{in}^N(t_T) \end{bmatrix} \begin{bmatrix} a_1 \\ a_2 \\ \vdots \\ a_N \end{bmatrix} = \begin{bmatrix} v_{out}(t_1) \\ v_{out}(t_2) \\ \vdots \\ v_{out}(t_N) \end{bmatrix}$$

Figure 2.28: The matrix representation of the equation 2.25 [7]

The equation 2.25 for the general case can be expressed as  $\mathbf{y} = \mathbf{H}\mathbf{x}$ , where  $\mathbf{H}$  is a  $M \times N$  matrix and  $M > N$  denotes that the number of rows (observations) is substantially more than the number of coefficients. The easiest way to approximate the vector  $\mathbf{x}$  in this case is to use least squares estimation, even though there are theoretically infinitely many possible solutions. The solution for this matrix equation is represented as:

$$\mathbf{x} = (\mathbf{H}^H\mathbf{H})^{-1}\mathbf{H}^H\mathbf{y} \quad (2.26)$$

Equation 2.26 is known as the Normal equation and the expression  $\mathbf{H}^\dagger = (\mathbf{H}^H\mathbf{H})^{-1}\mathbf{H}^H$  is called the pseudo-inverse [1].

# Chapter 3

## Behavioral Modeling of Power Amplifiers

### 3.1 Behavioral Models

In order to compensate for distortions using DPD, finding accurate models of the PA is quite essential . From system identification aspect, based on the data type that is required to be extracted and identified , PA models can be categorized into two major groups : Empirical and physical models. Physical models give an accurate description of a device based on fundamental physical laws meaning that in circuitry models, electrical components and circuit theory are used to model the system. Such techniques have high precision which is dependent to the quality of the device models resulting in a high cost and difficulties for simulation. Additionally, It will also be very difficult to create an inverse circuit model for compensating the nonlinear effects[3]. Empirical models, on the other hand benefits from simulating the system without any prior knowledge of the device internal circuitry. They are made of the sampled measured input and output signals , and they are also known as behavioral models or black-box models [3]. These kind of models are frequently used for DPD because of how simple they are to create and how quickly they simulate and process data. The fundamentals of PA modeling and the behavioral models for DPD utilized in this thesis are presented in this chapter. According to [PDF], the BM can be classified in three main categories that are summarized in figure 3.1.

Memory type	PA characteristics	Modeling method	
Memoryless	only include AM/AM distortion	Taylor series	no phase changes
Quasi-Memoryless	Frequency-Independent: -AM/AM distortion. -AM/PM distortion.	-Complex Power Series. -Polynomial model. -Saleh Model.	Short-term Memory Effects
Memory	Frequency-dependent: -AM/AM distortion. -AM/PM distortion.	-Volterra Series. -Wiener. -Hammerstein.	Long-term Memory Effects

Figure 3.1: Classification of memory effects for the Behavioral Modeling of nonlinear RF PA . Unlike the AM/AM characteristic, which is always observed in any nonlinear device, phase distortion is only observed in dynamic devices such as PAs that contain memory[2]

There are simplified versions such as Hammerstein model, Wiener model, Generalized Memory Polynomial, and Memory Polynomial model. Specifically, the Saleh model, the Memoryless MP model, the MP model, and the GMP model are examined in this thesis. Models should be adapted to new PAs with new tracking schemes to maintain high accuracy. Therefore, even if a model performs well with MAX PAE ET, it may not perform well with MAX PAE PET. Therefore, the parameters in figure 2.23 that are selected as the preset parameters should be chosen carefully so as to meet the expectations for each model.

## 3.2 Preparation of Model

Predistortion involves two main steps: modeling and distortion. The summarized modeling procedure illustrates in Figure 3.2. To conduct the modeling procedure, first the baseband waveforms are acquired from the input and output which are then followed with selecting of an appropriate model [6]. In the next step, an identification procedure is conducted to identify the parameters of the selected model by minimizing the differences between the mathematical description and the actual behavior of the PA. Finally, the modeling process is validated.

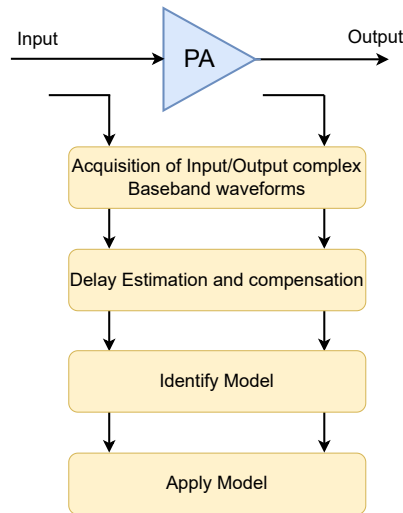


Figure 3.2: BM extraction procedure: key steps from measurements to model validation [6]

## 3.3 Volterra Model

The most complete model for dynamic nonlinear systems is the Volterra model. The input and output waveforms in this model have the following expression[6]:

$$x_{out}(n) = \sum_{k=1}^K \sum_{i_1=0}^M \sum_{i_p=0}^M h_p(i_1, \dots, i_p) \prod_{j=1}^k x_{in}(n - i_j) \quad (3.1)$$

where the Volterra model parameters are  $h_p(i_1, \dots, i_p)$ , its nonlinearity order is  $K$ , and its memory depth is  $M$ . With the nonlinearity order and the memory depth,

the number of parameters in the conventional Volterra series dramatically rises which in turn restricted the practical use of the Volterra series to weakly nonlinear systems with low-order nonlinearity. Figure 3.3 compare the complexity vs. performance of some BMs.

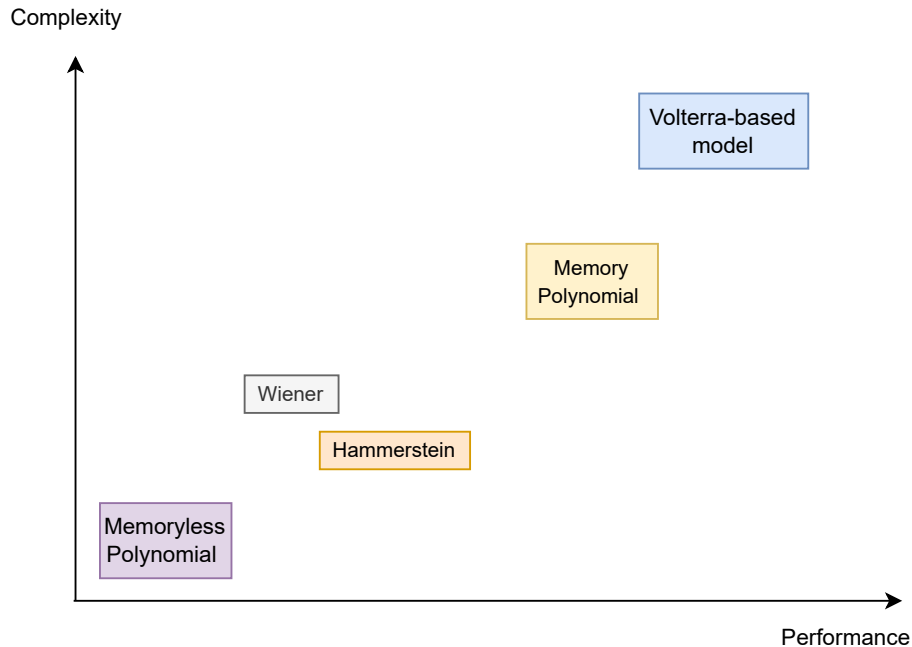


Figure 3.3: Trade-off between complexity and performance of the different models such as block-oriented models (Hammerstein and Wiener) and MP that are the simplified version of the Volterra model.

Numerous methods to simplify the Volterra series model have been suggested in helping to reduce this complexity. When modeling weakly nonlinear PAs, models built based on the Volterra series show excellent accuracy. These models may be more complex (in terms of the number of parameters) for strongly nonlinear PAs than other state-of-the-art models while still achieving a comparable performance [3]. The most popular method for obtaining BMs from the Volterra series is to identify and construct the model based on the most important terms within the series resulting in reduced Volterra series models.

### 3.4 Memoryless Nonlinear Model

For the memoryless models, it is assumed that the output envelope, responds instantaneously to changes in the input envelope and, as a result, assumes static AM/AM and AM/PM characteristics. As a result, they can be described by two algebraic functions of the instantaneous envelope amplitude that describe the real and imaginary output envelope components, or, more commonly, their amplitude and phase. Two commonly used examples of equivalent memoryless models are the Complex Power Series and the Saleh model.

### 3.4.1 Saleh Model

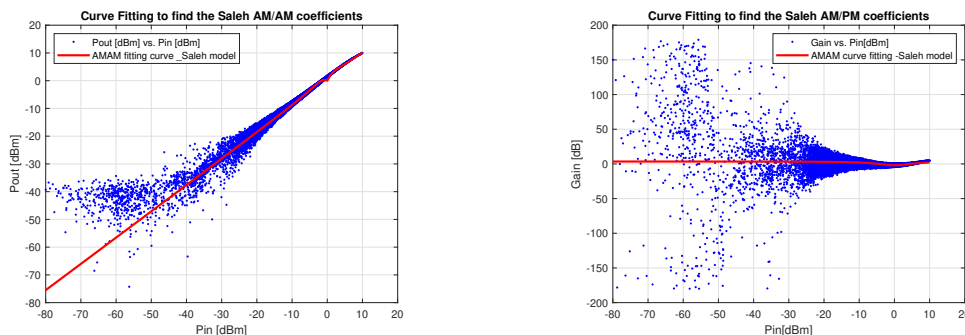
The Saleh model describes the memoryless nonlinearity (as mentioned in figure 3.1, it is categorised as the quasi-memoryless model). Equation 3.2 defines the magnitude of PA output,  $A(r)$ , in relation to the normalized input magnitude and is known as AM/AM characteristic function.

$$A(r) = \frac{\alpha_a r}{1 + \beta_a r^2} \quad (3.2)$$

Equation 3.3 defines the PA output phase,  $\Phi(r)$ , in relation to the normalized input magnitude and it is known as the AM/PM characteristic function [3].

$$\Phi(r) = \frac{\alpha_\phi r^2}{1 + \beta_\phi r^2} \quad (3.3)$$

The coefficients  $\alpha_a$ ,  $\beta_a$ ,  $\alpha_\phi$  and  $\beta_\phi$  are the fitting parameters to the measured PA AM/AM and AM/PM characteristics. An example of using of the curve fitting is illustrated in figure 3.4.



(a) AM/AM characteristic. The red line is used to find the coefficients  $\alpha_a$ ,  $\beta_a$ . (b) AM/PM characteristic. The red line is used to find the coefficients  $\alpha_\phi$  and  $\beta_\phi$ .

Figure 3.4: The AM/AM and AM/PM characteristics of the PA.

For better curve fitting, this MATLAB toolbox offers optimized solver parameters and starting conditions [16]. Figure 3.5 illustrates this useful toolbox, which enables the curve fitting process according to the user-defined functions, making it suitable to determine the Saleh model's coefficients.

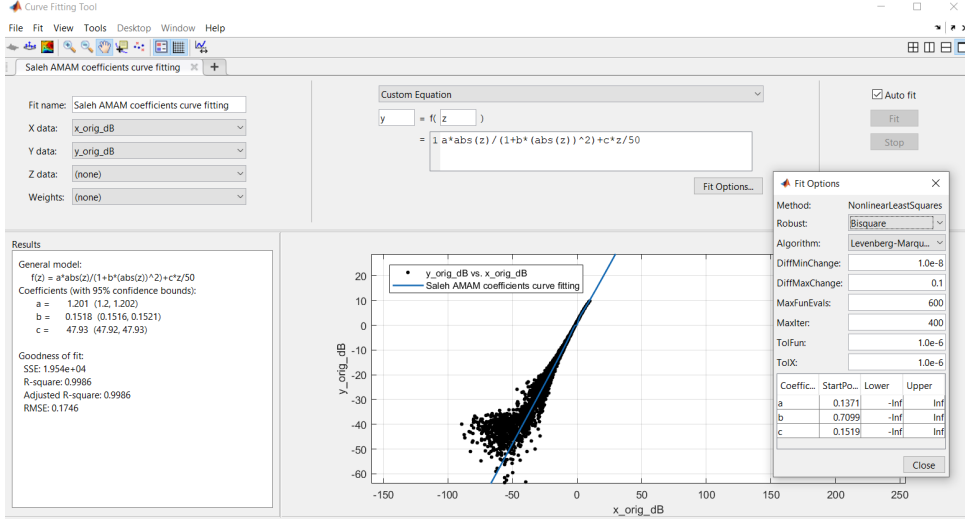


Figure 3.5: The MATLAB curve fitting toolbox to find the Saleh's Coefficients.

## 3.5 Nonlinear Models with Nonlinear Memory

### 3.5.1 Generalized Memory Polynomial Model(GMP)

A generalized memory polynomial model is built by augmenting the memory polynomial model with additional basis functions, which introduce cross-terms resulting from combining the instantaneous complex signal with leading and lagging terms. According to this model, the output  $y[n]$  and the input  $x[n]$  relationship can be expressed as [1]:

$$\begin{aligned}
 y[n] = & \sum_{p=0}^{K_a} \sum_{l=0}^{M_a} a_{p,l} x[n-m] |x[n-m]|^p \\
 & + \sum_{p=1}^{K_b} \sum_{l=0}^{L_b} \sum_{m=1}^{M_b} b_{p,l,m} x[n-l] |x[n-l-m]|^p \\
 & + \sum_{p=1}^{K_c} \sum_{l=0}^{L_c} \sum_{m=1}^{M_c} c_{p,l,m} x[n-l-m] |x[n-l]|^p \quad (3.4)
 \end{aligned}$$

The GPM output is composed of three polynomial functions. The first has a nonlinearity order and memory depth of  $K_a$  and  $L_a$ , respectively, and is applied to time-aligned input signal samples. The complex input signal and lagging values of its envelope are exposed to the second polynomial function. With a nonlinearity order of  $K_b$  and a memory depth of  $M_b$ , this polynomial function introduces cross-terms between the input signal and its lagging envelope terms up to the  $L_b$  order[17]. The third polynomial function also introduces cross-terms between the input signal and the leading envelope terms up to the  $L_c$  order. The leading cross-terms polynomial has  $K_c$  and  $M_c$  as its nonlinearity order and memory depth, respectively. In the equation 3.4,  $a_{p,l}$ ,  $b_{p,l,m}$ , and  $c_{p,l,m}$  are the coefficients of the memory polynomial functions applied to the aligned terms, the lagging cross-terms, and the leading cross-terms, respectively[18].

### 3.5.2 Memory Polynomial Model(MP)

By reducing the Volterra series model down to its diagonal terms( or by eliminating all cross-terms), MP model can be achieved. The baseband complex output signal  $y[n]$  of the MP model is expressed as a function of its baseband complex input signal  $x$  according to[1]:

$$y[n] = \sum_{p=0}^{K_a} \sum_{m=0}^{M_a} c_{p,m} x[n-m] |x[n-m]|^p \quad (3.5)$$

where  $c_{p,m}$  denotes for the model coefficients,  $K_a$  is the nonlinearity order, and  $M_a$  indicates the memory depth. It can be noticed that the equation 3.5 is equal to the first term in the equation 3.4 .



# Chapter 4

## Implementation and Results

### 4.1 Setup

The connection of the measurement equipment is shown in Figure 4.1. The instruments used to make the measurements are listed in table 4.1. As can be seen, the circulator is connected to the driving PA in such a way that the signal only passes in one direction to the PA of interest. There are also two ARBs, one of which is connected to the RF source to upconvert the I/Q signal to a single RF signal and the other of which is used to track the drain when the DPD is tested using ET or PET[8]. After amplification, the signal passes through a directional coupler with a suitable amount of loss to ensure that its power does not exceed the signal analyzer's maximum input. A reference clock is used to synchronize the spectrum analyzer, the two ARBs, and the RF source. Then, all the parameters were stored as a structure file( .m file )in MATLAB. the table 4.3 contains the measured values for 5 different PAs with the different tracking schemes.

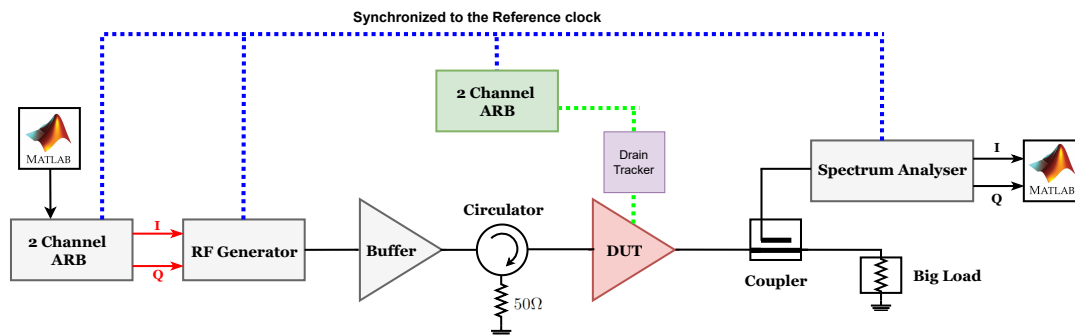


Figure 4.1: The measurement setup[2]

<b>Device</b>	<b>Model</b>	<b>Producer</b>
Arbitrary Waveform	33600A	KEYSIGHT
RF Source	SGS100A	Rohde & Schwarz
Oscilloscope	RTE 1054	Rohde & Schwarz
Spectrum Analyzer	FSVA3013	Rohde & Schwarz

Table 4.1: The instrument used for the measurements[8].

A list of the input signal parameters is given in table 4.2. In addition, there are 20 empty symbols were put at the start and end of each data sequence. Figure 4.2 illustrates the PSD of the 5 different PAs without DPD and the input signal. The Spectral Regrowth can be seen for all of them comparing to the input signal.

<b>Parameter</b>	<b>Value</b>
<b>RF Frequency</b>	2 GHz
<b>Modulation</b>	16QAM
<b>Symbol Rate</b>	3.84 Msymb/s
<b>Number of Symbols</b>	10000
<b>Oversampling Factor</b>	64
<b>Roll-off</b>	0.22
<b>Sampling rate(<math>f_s</math>)</b>	245MHz

Table 4.2: Input signal parameters [8].

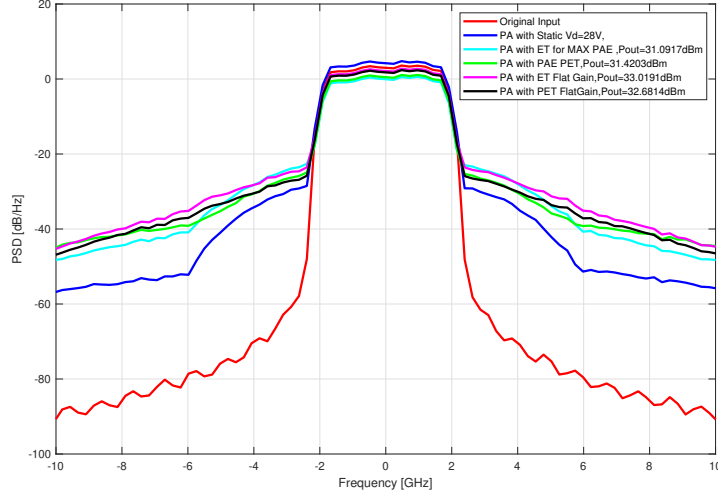


Figure 4.2: The PSD of output signals for PAs with different tracking schemes, without DLA DPD.

Tracking scheme	ACPR[dB]	EVM[%]	NMSE[dB]	STDR[dB]	$P_{out}$ [dBm]
Static Vd=28	[-38.673,-39.155]	3.427	-28.661	28.663	33.406
MAX PAE	[-28.406,-28.549]	8.952	-19.291	19.304	31.091
MAX PAE PET	[-31.017,-31.280]	6.873	-21.968	21.976	31.420
Flat Gain=12dB	[-30.432,-30.357]	7.636	-21.916	21.924	33.019
Flat Gain PET=12dB	[-32.282,-32.241]	5.858	-23.775	23.780	32.681

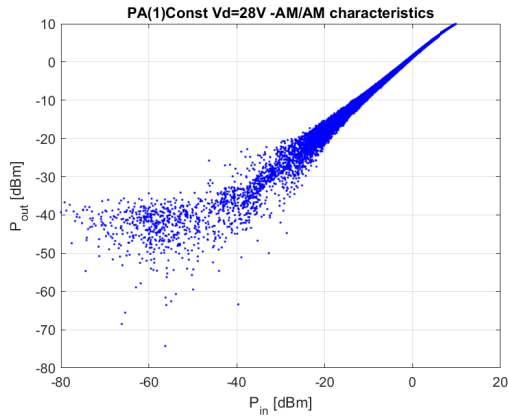
Table 4.3: Measured specifications of 5 different PAs at  $f=2.0$ GHz with the different tracking schemes, without DPD.

## 4.2 Results

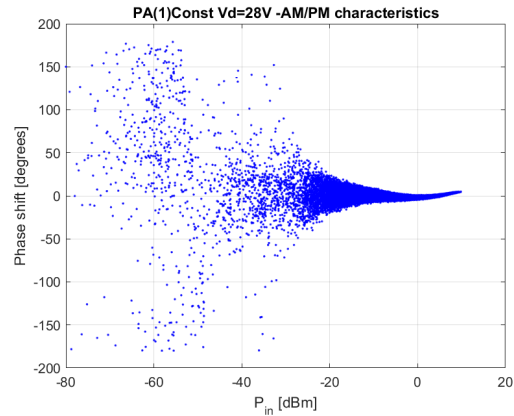
In this section, the AM/AM and AM/PM characteristics, AM/AM normalized scaled and gain of the different PAs are illustrated. The results of implementing DLA DPD using the MP and GMP are summarized for each PA. After that, the results are compared and the best model that improves performance is explained.

### 4.2.1 PA with Constant (static) Drain Voltage $V_d=28$ V

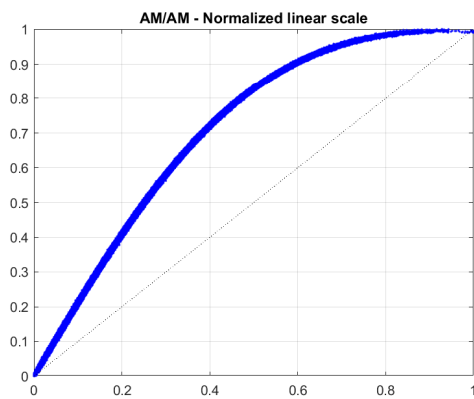
For all input envelope values, the drain voltage for the PA is maintained at 28V [8]. A 16-QAM input is measured at a distinct average output power level, where the peaks of the modulated signal reach compression at different degrees, in order to verify the PA behavior with a linearization method. This information is then utilized to fit the DLA DPD. Figure 4.3 illustrates the AM/AM, AM/PM characteristics, the AM/AM normalized linear scale and EVM for the PA with constant  $V_d=28$ V before applying the DLA DPD.



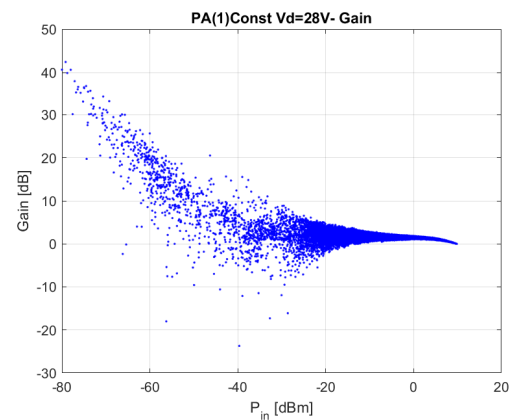
(a) AM/AM characteristic of PA with static  $V_d=28V$ , without DLA DPD



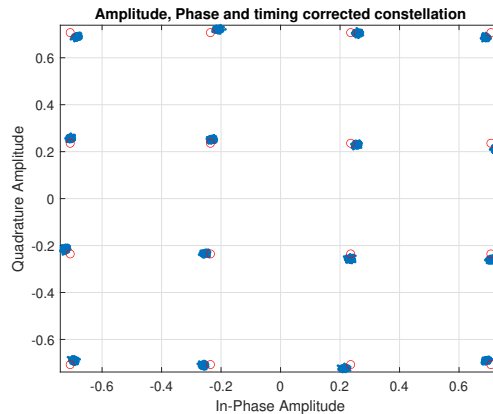
(b) AM/PM characteristic of PA with static  $V_d=28V$ , without DLA DPD



(c) AM/AM normalized linear scale of PA with static  $V_d=28V$ , without DLA DPD



(d)  $P_{in}$  vs gain ,witout DLA DPD



(e)  $EVM=3.427$  ,Without DLA DPD

Figure 4.3: Results of simulation for the PA with static  $V_d=28V$ , without DLA DPD

Table 4.4 ,shows the Linearization results for PA with the constant Drain voltage .For the first scenario it assumed that the memory length is set to 0 ,while the polynomial order changes. Notice that when the  $M_a$  in the expression 3.5 sets to 0 ,the  $M_a$  model can be seen as a model without memory effect,while by setting  $M_a$  to a certain value,the MP can simulates the PA with the memory effect.the  $M_a$  is

referred to the memory depth.

Model	ACPR[dB]	EVM[%]	NMSE[dB]	STDR[dB]	$P_{out}[dBm]$
Without DPD	[-38.673,-39.155]	3.427	-28.661	28.663	33.406
$MP^{pol.order=5}_{mem.depth=0}$	[-53.406,-53.609]	0.871	-42.809	42.814	33.317
$MP^{pol.order=10}_{mem.depth=0}$	[-53.470,-53.679]	0.680	-42.855	42.860	33.321
$MP^{pol.order=15}_{mem.depth=0}$	[-53.512,-53.700]	0.827	-42.882	42.886	33.325

Table 4.4: Results of measurements for PA with constant drain voltage after applying the Memoryless DPD.

Table 4.4 represents the results of MP DPD by applying different polynomial orders while keeping the memory depth equals to 0. The model achieving the overall greatest linearization is the  $MP^{pol.order=15}_{mem.depth=0}$ , here the EVM is reduced with 2.6%, and the ACPR reduced dramatically with 17.439dB for the lower ACPR and 14.545dB for the upper ACPR. The improvements in NMSE and STDR are measured to be 14.221 dB and 14.223 dB respectively. Thus, the  $MP^{pol.order=15}_{mem.depth=0}$  DPD significantly improves both EVM and ACPR .

When considering the memory depth for the MP model with different polynomial orders, the results for the MP DPD are summarized in table 4.5.

Model	ACPR[dB]	EVM[%]	NMSE[dB]	STDR[dB]	$P_{out}[dBm]$
Without DPD	[-38.673,-39.155]	3.427	-28.661	28.663	33.406
$MP^{pol.order=5}_{mem.depth=3}$	[-53.442,-53.654]	1.130	-42.820	42.823	33.328
$MP^{pol.order=10}_{mem.depth=5}$	[-53.492,-53.644]	0.678	-42.850	42.852	33.354
$MP^{pol.order=15}_{mem.depth=7}$	[-53.534,-53.750]	0.775	-42.890	42.895	33.340

Table 4.5: Results of measurements for PA with constant drain voltage after applying the MP DPD.

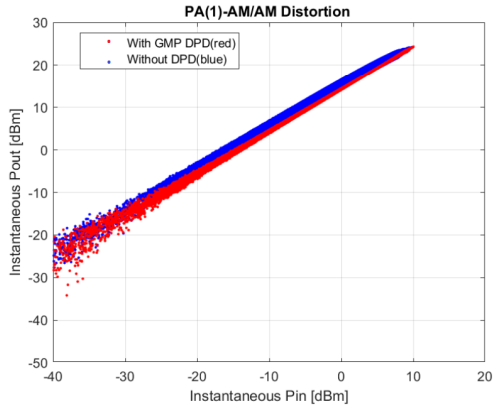
As it can be seen ,the best FoM improvement among the MP in table 4.5 can be achieved by  $MP^{pol.order=15}_{mem.depth=7}$  DPD ,with reducing the ACPR by 14.861dB and 14.595dB, and after the DPD iteration,the SDTR is improved by 14.232dB.

For the PA with static  $V_d=28V$ ,the results of implementing DLA DPD with GMP model are presented in table 4.6.

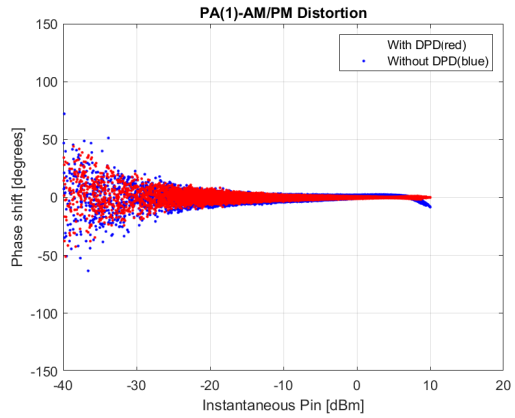
Model	ACPR[dB]	EVM[%]	NMSE[dB]	STDR[dB]	$P_{out}$ [dBm]
Without DPD	[-38.673,-39.155]	3.427	-28.661	28.663	33.406
$GMP_{mem.depth=5}^{pol.order=5}$	[-53.454,-53.650]	0.735	-42.838	42.842	33.361
$GMP_{mem.depth=5}^{pol.order=10}$	[-53.544,-53.750]	0.883	-42.897	42.900	33.311
$GMP_{mem.depth=7}^{pol.order=15}$	[-53.517,-53.715]	1.052	-42.892	42.895	33.340
$GMP_{mem.depth=17}^{pol.order=20}$	[-53.560,-53.735]	0.844	-42.910	42.913	33.322

Table 4.6: Results of measurements for PA with constant drain voltage after applying the GMP DPD.

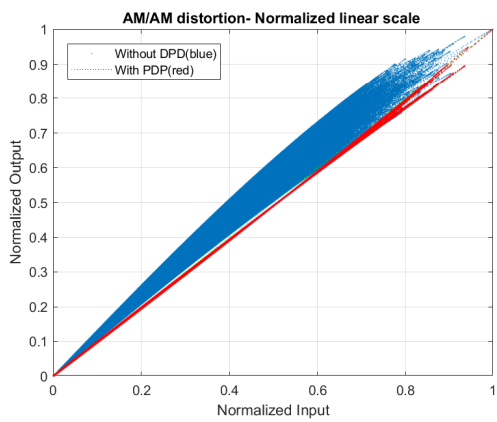
Among the different implemented GMP models with different polynomial order and memory depth represented in table 4.6, the  $GMP_{mem.depth=17}^{pol.order=20}$  shows the best results with a huge reduction of 14.887dB, 14.580dB for the ACPR, and the STDR enhancement of 14.250 dB. However, the GMP model utilizes a lot of terms to perform DPD at the cost increasing the computational time. This verifies the trade off between complexity and performance of the model, that explained in the section 3.3. The results after applying the DLA DPD for the PA with constant  $V_d=28V$  are illustrated in figure 4.4.



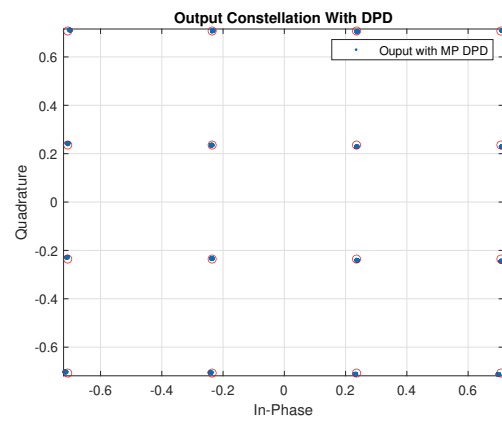
(a) AM/AM characteristic of PA with DPD,without DPD



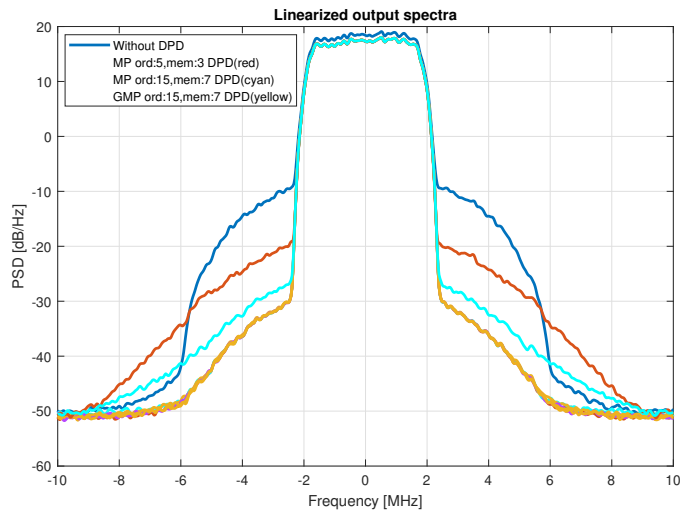
(b) AM/PM characteristic of PA with DPD,without DPD



(c) AM/AM normalized linear scale without DPD and with DPD



(d) EVM=0.928 After DPD

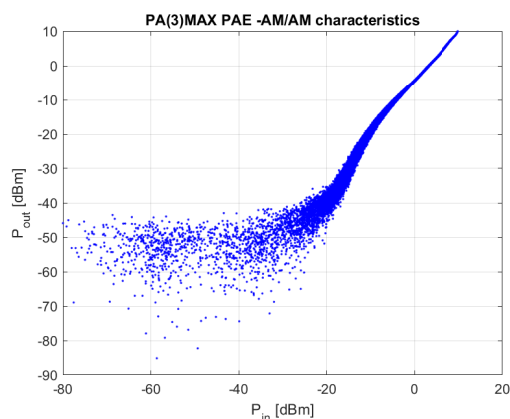


(e) PSD without DPD,with MP DPD and with GMP DPD

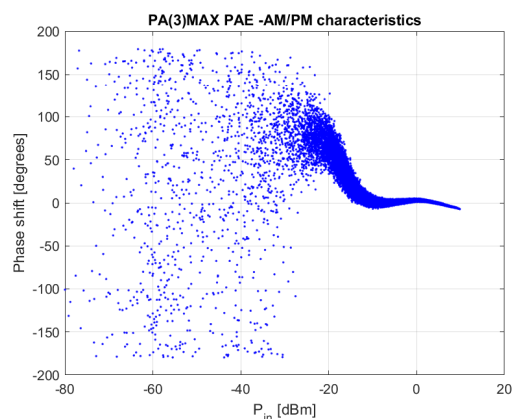
Figure 4.4: Results of simulation for a memoryless PA ,with DLA DPD.

## 4.2.2 PA Combined with MAX PAE Tracking Scheme

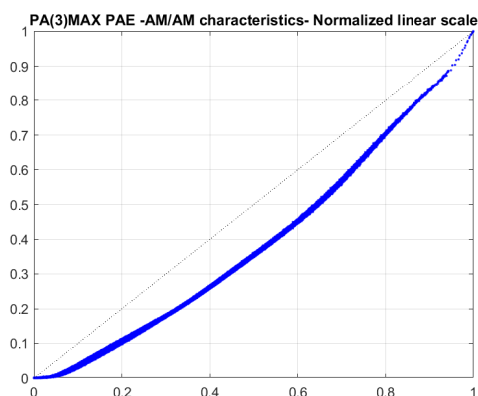
Figure 4.5 illustrates the AM/AM, AM/PM characteristics, the AM/AM normalized linear scale and EVM for the PA with MAX PAE tracking scheme before applying the DLA DPD.



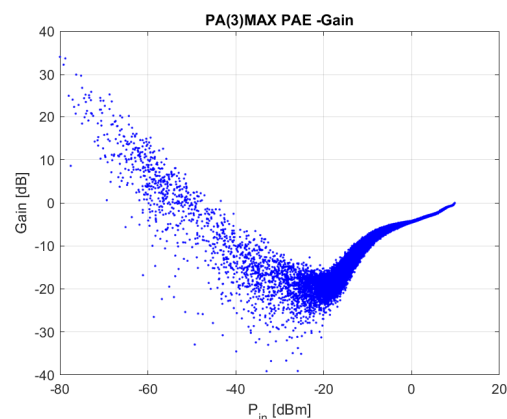
(a) AM/AM characteristic of PA with MAX PAE tracking.



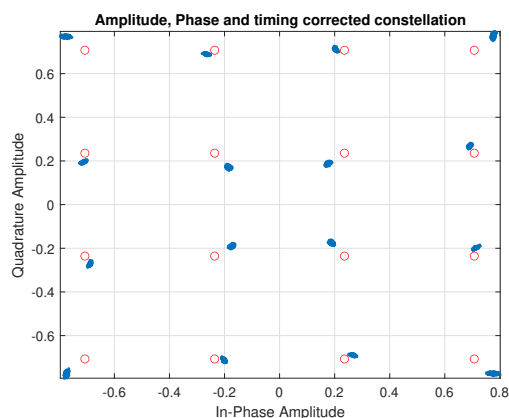
(b) AM/PM characteristic of PA with MAX PAE tracking.



(c) AM/AM normalized linear scale of PA with MAX PAE



(d)  $P_{in}$  vs Gain of PA MAX PAE, without DLA DPD



(e) EVM=8.952, Without DLA DPD

Figure 4.5: Results of simulation for the PA with MAX PAE tracking, without DLA DPD



The results for the DLA DPD combined with the PA that optimized for tracking maximum PAE are presented in tables 4.7,4.8, 4.9 corresponding to the Memoryless MP ,MP and GMP models respectively.

Model	ACPR[dB]	EVM[%]	NMSE[dB]	STDR[dB]	$P_{out}[dBm]$
Without DLA DPD	[-28.406,-28.549]	8.952	-19.291	19.304	31.091
$MP^{pol.order=5}_{mem.depth=0}$	[-41.745,-41.692]	2.535	-32.527	32.531	34.160
$MP^{pol.order=10}_{mem.depth=0}$	[-36.466,-36.458]	2.202	-28.578	28.602	34.445
$MP^{pol.order=15}_{mem.depth=0}$	[-38.322,-38.336]	2.173	-29.819	29.912	33.689

Table 4.7: Results of measurements for PA MAX PAE after applying the Memoryless DPD.

Comparing the results from the tables 4.7 , 4.8, and 4.9, it can be deduced that  $MP^{pol.order=5}_{mem.depth=3}$  has the best improvements, which correspond to the ACPR with 12,208dB, 12,146dB, and 14,61dB of STDR modification, while NMSE improvement was best for  $MP^{pol.order=15}_{mem.depth=3}$ , and the best correction for EVM is related to  $GMP^{pol.order=20}_{mem.depth=17}$  with 7.287% correction.

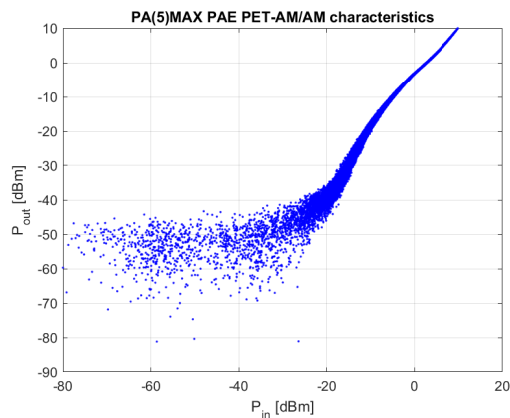
Model	ACPR[dB]	EVM[%]	NMSE[dB]	STDR[dB]	$P_{out}[dBm]$
Without DLA DPD	[-28.406,-28.549]	8.952	-19.291	19.304	31.091
$MP^{pol.order=5}_{mem.depth=3}$	[-44.933,-44.927]	2.458	-33.909	33.914	33.054
$MP^{pol.order=10}_{mem.depth=5}$	[-37.705,-37.722]	2.097	-29.572	29.586	33.798
$MP^{pol.order=15}_{mem.depth=7}$	[-40.614,-40.695]	2.104	-31.419	31.429	32.940

Table 4.8: Results of measurements for PA MAX PAE after applying the MP DPD.

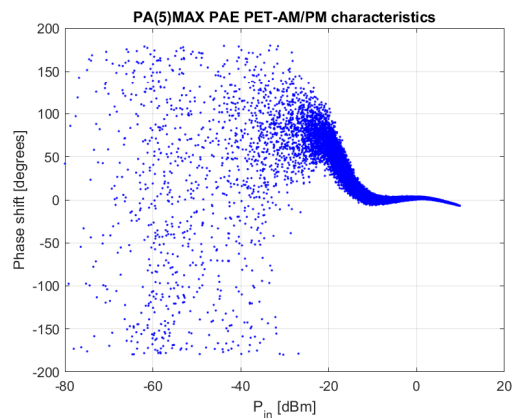
Model	ACPR[dB]	EVM[%]	NMSE[dB]	STDR[dB]	$P_{out}[dBm]$
Without DLA DPD	[-28.406,-28.549]	8.952	-19.291	19.304	31.091
$GMP^{pol.order=5}_{mem.depth=5}$	[-39.665,-39.706]	2.120	-30.898	30.916	32.913
$GMP^{pol.order=10}_{mem.depth=5}$	[-36.044,-36.097]	1.735	-28.019	28.066	34.583
$GMP^{pol.order=15}_{mem.depth=7}$	[-33.385,-33.430]	2.214	-25.574	25.681	36.090
$GMP^{pol.order=20}_{mem.depth=17}$	[-35.896,-35.934]	1.665	-27.924	27.977	34.696

Table 4.9: Results of measurements for PA MAX PAE after applying the GMP DPD.

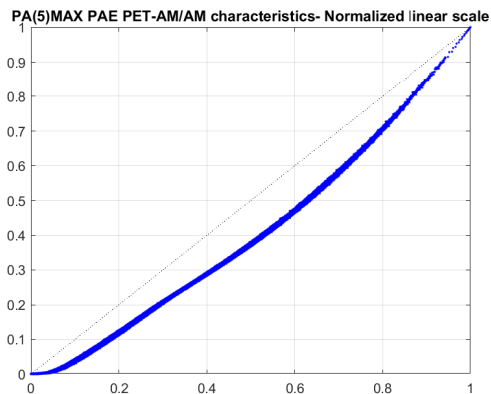
### 4.2.3 PA Combined with Max PAE PET Tracking Scheme



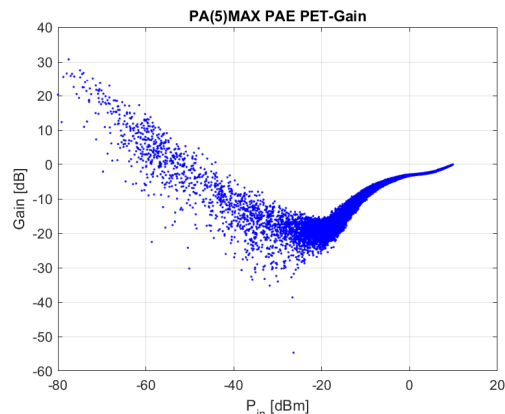
(a) AM/AM characteristic of PA with MAX PAE PET tracking.



(b) AM/PM characteristic of PA with MAX PAE PET tracking.



(c) AM/AM normalized linear scale of PA with MAX PAE PET, without DPD



(d)  $P_{in}$  vs Gain of PA MAX PAE PET, without DLA DPD

Figure 4.6: Results of simulation for the PA with MAX PAE PET tracking, before DLA DPD

Model	ACPR[dB]	EVM[%]	NMSE[dB]	STDR[dB]	$P_{out}$ [dBm]
Without DLA DPD	[-31.017,-31.280]	6.873	-21.968	21.976	31.420
MP <sup>pol.order=5</sup> <sub>mem.depth=0</sub>	[-41.103,-41.049]	2.665	-32.143	32.147	34.995
MP <sup>pol.order=10</sup> <sub>mem.depth=0</sub>	[-37.148,-37.138]	2.182	-29.135	29.153	34.708
MP <sup>pol.order=15</sup> <sub>mem.depth=0</sub>	[-34.276,-34.285]	2.436	-26.474	26.551	36.252

Table 4.10: Results of measurements for PA MAX PAE PET after applying the Memoryless DPD.

Model	ACPR[dB]	EVM[%]	NMSE[dB]	STDR[dB]	$P_{out}$ [dBm]
Without DLA DPD	[-31.017,-31.280]	6.873	-21.968	21.976	31.420
$MP_{mem.depth=3}^{pol.order=5}$	[-40.009,-39.970]	2.699	-31.386	31.390	35.302
$MP_{mem.depth=5}^{pol.order=10}$	[-37.278,-37.301]	2.209	-29.239	29.256	34.660
$MP_{mem.depth=7}^{pol.order=15}$	[-38.083,-38.153]	1.825	-29.694	29.717	34.433

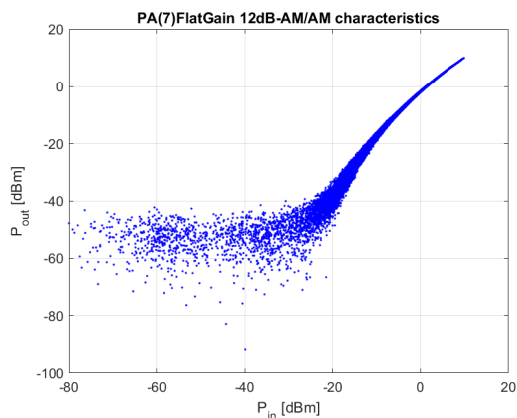
Table 4.11: Results of measurements for PA MAX PAE PET after applying the MP DPD.

Comparing the results from the tables 4.10 , 4.11, and 4.12, it can be seen that  $MP_{mem.depth=0}^{pol.order=5}$  has the best improvements, which correspond to the ACPR with 10.086dB, 9.769dB, and STDR correction of 10.171dB and NMSE improvement of 10.175dB, while the best correction for EVM is related to  $GMP_{mem.depth=5}^{pol.order=10}$  with 5.141% correction.

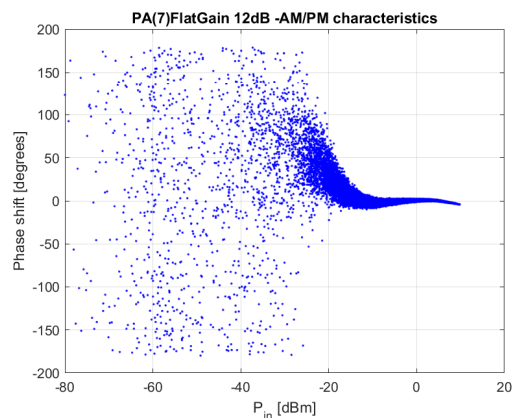
Model	ACPR[dB]	EVM[%]	NMSE[dB]	STDR[dB]	$P_{out}$ [dBm]
Without DLA DPD	[-31.017,-31.280]	6.873	-21.968	21.976	31.420
$GMP_{mem.depth=5}^{pol.order=5}$	[-38.696,-38.737]	2.202	-30.225	27.105	33.844
$GMP_{mem.depth=5}^{pol.order=10}$	[-36.435,-36.481]	1.732	-28.341	28.390	35.042
$GMP_{mem.depth=7}^{pol.order=15}$	[-34.141,-34.187]	2.135	-26.300	26.388	36.254
$GMP_{mem.depth=17}^{pol.order=20}$	[-38.162,-38.226]	1.954	-29.800	29.824	34.412

Table 4.12: Results of measurements for PA MAX PAE PET after applying the GMP DPD.

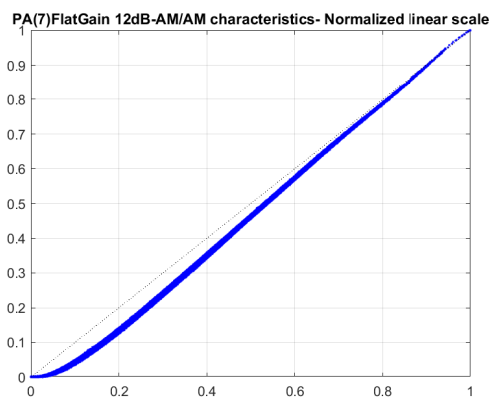
#### 4.2.4 PA Optimized with ET for tracking Flat Gain =12dB



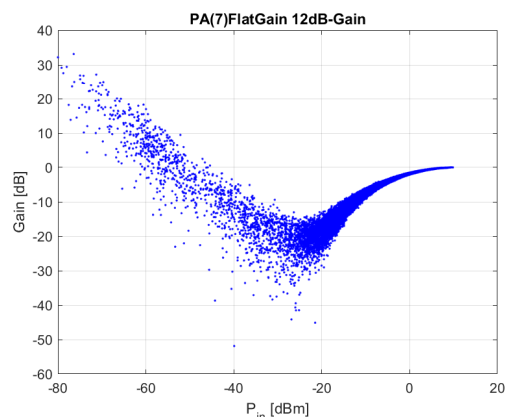
(a) AM/AM characteristic of PA with ET flat Gain=12dB.



(b) AM/PM characteristic of PA with ET flat Gain=12dB ,without DPD



(c) AM/AM normalized linear scale of PA with with ET flat Gain=12dB ,without DPD



(d)  $P_{in}$  vs Gain of PA with with ET flat Gain=12dB,without DLA DPD

Figure 4.7: Results of simulation for the flat gain PA with ET tracking, without DLA DPD

Model	ACPR[dB]	EVM[%]	NMSE[dB]	STDR[dB]	$P_{out}$ [dBm]
Without DLA DPD	[-30.432,-30.357]	7.636	-21.916	21.924	33.019
MP <sup>pol.order=5</sup> mem.depth=0	[-38.107,-38.046]	3.148	-30.033	30.037	33.223
MP <sup>pol.order=10</sup> mem.depth=0	[-36.374,-36.369]	2.187	-28.500	28.525	32.609
MP <sup>pol.order=15</sup> mem.depth=0	[-37.261,-37.283]	2.135	-26.075	29.105	32.237

Table 4.13: Results of measurements for PA ET flat gain=12dB after applying the Memoryless DPD.

Model	ACPR[dB]	EVM[%]	NMSE[dB]	STDR[dB]	$P_{out}[dBm]$
Without DLA DPD	[-30.432,-30.357]	7.636	-21.916	21.924	33.019
$MP^{pol.order=5}_{mem.depth=3}$	[-41.770,-41.735]	2.563	-32.512	32.516	32.280
$MP^{pol.order=10}_{mem.depth=5}$	[-35.663,-35.713]	2.431	-27.876	27.911	33.070
$MP^{pol.order=15}_{mem.depth=7}$	[-35.256,-35.329]	1.783	-27.365	27.425	33.215

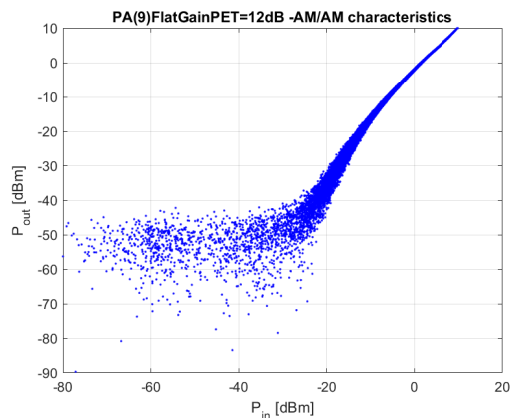
Table 4.14: Results of measurements for PA ET flat gain=12dB after applying the MP DPD

Comparing the results from the tables 4.13 , 4.14, and 4.15, it can be seen that  $MP^{pol.order=5}_{mem.depth=3}$  has the best improvements, which correspond to the ACPR with 11.338dB, 11.378dB, and STDR correction of 10.592dB and NMSE modification of 10.596dB, while the best improvement for EVM is related to  $GMP^{pol.order=10}_{mem.depth=5}$  with 5.930% correction.

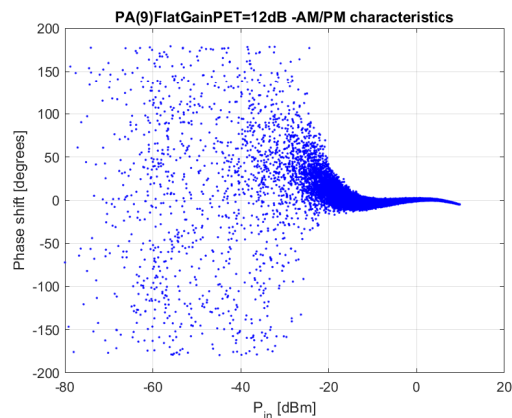
Model	ACPR[dB]	EVM[%]	NMSE[dB]	STDR[dB]	$P_{out}[dBm]$
Without DLA DPD	[-30.432,-30.357]	7.636	-21.916	21.924	33.019
$GMP^{pol.order=5}_{mem.depth=5}$	[-35.546,-35.593]	2.415	-27.687	27.719	32.594
$GMP^{pol.order=10}_{mem.depth=5}$	[-37.151,-37.203]	1.706	-28.936	28.971	32.207
$GMP^{pol.order=15}_{mem.depth=7}$	[-37.839,-37.878]	2.317	-29.490	29.518	32.596
$GMP^{pol.order=20}_{mem.depth=17}$	[-38.626,-38.694]	1.956	-30.143	30.163	31.710

Table 4.15: Results of measurements for PA ET flat gain=12dB after applying the GMP DPD

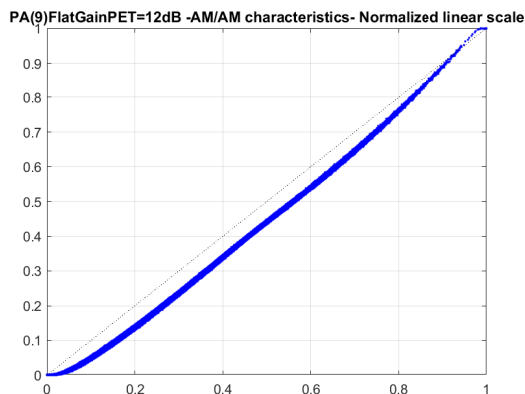
### 4.2.5 PA Optimized with PET Tracking Flat Gain =12dB



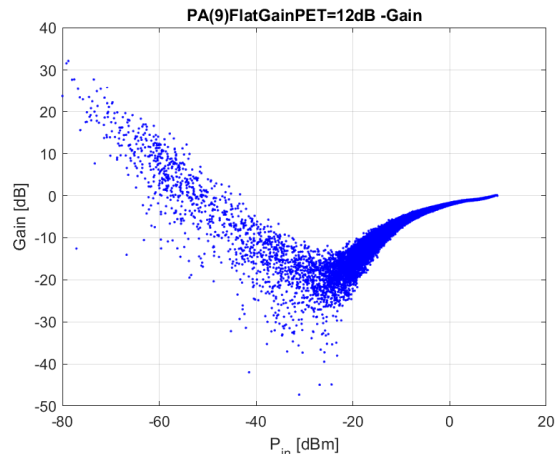
(a) AM/AM characteristic of PA with PET flat Gain=12dB.



(b) AM/PM characteristic of PA with PET flat Gain=12dB ,without DPD



(c) AM/AM normalized linear scale of PA with with PET flat Gain=12dB ,without DPD



(d)  $P_{in}$  vs Gain of PA with with PET flat Gain=12dB,without DLA DPD

Figure 4.8: Results of simulation for the flat gain PA with PET tracking, without DLA DPD

Model	ACPR[dB]	EVM[%]	NMSE[dB]	STDR[dB]	$P_{out}$ [dBm]
Without DLA DPD	[-32.282,-32.241]	5.858	-23.775	23.780	32.681
MP <sup>pol.order=5</sup> <sub>mem.depth=0</sub>	[-45.261,-45.263]	2.356	-34.001	34.007	31.124
MP <sup>pol.order=10</sup> <sub>mem.depth=0</sub>	[-36.511,-36.501]	1.914	-28.612	28.636	32.655
MP <sup>pol.order=15</sup> <sub>mem.depth=0</sub>	[-36.112,-36.129]	2.363	-28.126	28.171	32.899

Table 4.16: Results of measurements for PA PET flat gain=12dB after applying the Memoryless DPD

Model	ACPR[dB]	EVM[%]	NMSE[dB]	STDR[dB]	$P_{out}$ [dBm]
Without DLA DPD	[-32.282,-32.241]	5.858	-23.775	23.780	32.681
$MP^{pol.order=5}_{mem.depth=3}$	[-42.609,-40.582]	2.641	-32.972	32.976	32.147
$MP^{pol.order=10}_{mem.depth=5}$	[-36.244,-36.282]	2.113	-28.380	28.407	32.840
$MP^{pol.order=15}_{mem.depth=7}$	[-36.963,-37.032]	1.731	-28.823	28.856	32.498

Table 4.17: Results of measurements for PA PET flat gain=12dB after applying the MP DPD

Comparing the results from the tables 4.16 , 4.17, and 4.18, it can be seen that the memoryless  $MP^{pol.order=5}_{mem.depth=0}$  has the best improvements, which correspond to the ACPR with 12.979dB, 13.022dB, and STDR correction of 10.227dB and NMSE modification of 10.227dB, while the best improvement for EVM is related to  $GMP^{pol.order=20}_{mem.depth=17}$  with 4.151% correction.

Model	ACPR[dB]	EVM[%]	NMSE[dB]	STDR[dB]	$P_{out}$ [dBm]
Without DLA DPD	[-32.282,-32.241]	5.858	-23.775	23.780	32.681
$GMP^{pol.order=5}_{mem.depth=5}$	[-36.831,-36.807]	2.388	-28.773	28.798	32.112
$GMP^{pol.order=10}_{mem.depth=5}$	[-40.480,-40.547]	1.940	-31.391	31.404	31.227
$GMP^{pol.order=15}_{mem.depth=7}$	[-37.718,-37.762]	2.116	-29.398	29.427	32.168
$GMP^{pol.order=20}_{mem.depth=17}$	[-38.539,-38.608]	1.707	-30.079	30.100	31.867

Table 4.18: Results of measurements for PA PET flat gain=12dB after applying the GMP DPD

# Chapter 5

## Discussion

This chapter will concentrate on the most important results of applying DLA DPD using various PAs, which used diverse tracking schemes, and will compare the best parameter selections to use with the MP,GMP behavioral models for obtaining the best DPD results.

Regardless of the Behavioral Model used, such as GMP or MP, the utilization of a DLA DPD increases linearity, drastically reduces EVM and ACPR, and significantly increases STDR and NMSE across all measured values described in section 4.2 .All simulations employed the Saleh model as a synthetic PA. Thus, the significance of curve fitting in determining the Saleh model coefficients is once more emphasized. The coefficients that were obtained by curve fitting were not exact for PA with higher nonlinearity, such as PA used for MAX PAE ET and MAX PAE PET, leading to the mediocre results and the deviation of the simulated AM/AM and AM/PM characteristics from the measured AM/AM and AM/PM characteristics during the validation steps.

The Modified Saleh model, which includes more terms and more flexibility because of it, is probably a superior option because it makes it simpler to estimate the parameters, leading to findings that are more accurate. Although the results of applying the Saleh model to the PA with static drain voltage , which has a lower order of nonlinearity, were better than anticipated, it is likely that the Saleh model's coefficients could probably be modified for the PAs with HEMT technology .

Simulation results for PAs with higher nonlinearity orders also revealed that, in contrast to the memoryless models with lower polynomial orders, an increase in the memory depth or polynomial order did not always result in a significant improvement in ACPR or STDR ,but the best EVM corrections were achieved using GMP with greater memory depths.

In the other word, with the lower order nonlinearities, the memoryless MP DPD can linearize the PAs perfectly. However, the MP DPD provides the linearization of both static and dynamic nonlinearities for the PAs that have dynamic nonlinearities since it takes the memory effects of the PA into consideration.



# Chapter 6

## Conclusion

A DPD can be incorporated into a PA to improve the linearity of the system. The linearization techniques are explained briefly and the linearization method using MP DPD and GMP DPD are presented in this thesis. The Direct Learning Architecture was selected to perform DPD. Then, the performances of the memoryless DPD, MP DPD and GMP DPD over the 5 different PAs with different tracking schemes are compared and increase in linearization is shown by taking memory effects into account. The linearization results were achieved for all of the PAs that tested in this thesis as expected. The best results for PA with ET is obtained with  $MP_{mem.depth=3}^{pol.order=5}$ , while the best results for PA with PET is achieved by  $MP_{mem.depth=0}^{pol.order=5}$ . For the PA with flat gain, the best result is achieved by  $MP_{mem.depth=3}^{pol.order=5}$  for PA PE and  $MP_{mem.depth=0}^{pol.order=5}$  for PA PET. However the best EVM results are achieved by  $GMP_{mem.depth=5}^{pol.order=10}$ .

# Bibliography

- [1] J. A. Becerra and M. J. Madero-Ayora, “DPD and Sparse Estimation . IEEE Radio and Wireless Week.Las Vegas, NV, USA,” Jan. 2022.
- [2] B. Eskandariturk, “Implementation of Digital Predistortion for RF/Microwave transmitters.,” *NTNU*, Dec. 2021.
- [3] D. Schreurs, A. A. GOACHER, and M. GADRINGER, *RF Power Amplifier Behavioral Modeling*. CAMBRIDGE UNIVERSITY PRESS, first ed., 2008.
- [4] F. Li, “Linearization of Power Amplifiers in Wideband Communication Systems by Digital Baseband Dredistortion Technique.,” *UNIVERSITE DE NANTES*, 2012.
- [5] P. B. Kenington, *High Linearity RF Amplifier design*. London: Artech House, 2000.
- [6] F. M. Ghannouchi and O. Hammi, “Behavioral Modeling and Predistortion,” *IEEE Microwave Magazine*, Dec. 2009.
- [7] J. Wood, *Behavioral Modeling and Linearization of RF Power Amplifiers*. London: ARTECH HOUSE, INC., 2014.
- [8] S. Eika, “Implementation of Digital Predistortion for RF/Microwave transmitters,” *NTNU*, July 2020.
- [9] G. ERDOGDU, “Linearization of RF Power Amplifiers by using Memory Polynomial Digital Predistortion Technique,” *THE GRADUATE SCHOOL OF NATURAL AND APPLIED SCIENCES OF MIDDLE EAST TECHNICAL UNIVERSITY*, June 2012.
- [10] M. Olavsbråten, “TFE4595 Electronic Systems Design, fordypningsemne. [https://ntnu.blackboard.com/ultra/courses/\\_30045\\_1/cl/outline](https://ntnu.blackboard.com/ultra/courses/_30045_1/cl/outline),” 2021.
- [11] D. M. Pozar, *Microwave Engineering*. JohnWiley &Sons, 4th edition ed., 2012.
- [12] M. Bache, “Digital Predistortion Linearization of Power Amplifier for X-band Radar System,” *NTNU*, July 2015.
- [13] K. M. Gharaibeh, *Nonlinear Distortion in Wireless Systems. Modeling and Simulation With MATLAB*. Yarmouk University, Jordan: John Wiley & Sons Ltd, 2012.

- [14] D. Gecan, K. M. Gjertsen, and M. Olavsbråten, “Novel Metric Describing Total Nonlinearity of Power Amplifier With a Corresponding Figure of Merit for Linearity Evaluation and Optimization,” *IEEE MICROWAVE AND WIRELESS COMPONENTS LETTERS*, vol. 27, Jan. 2017.
- [15] M. Olavsbråten and D. Gecan, “Bandwidth Reduction for Supply Modulated RF PAs using Power Envelope Tracking,” *IEEE Microwave and Wireless Components Letters*, vol. 27, 2017.
- [16] h. The MathWorks, Inc, “Curve Fitting Toolbox,” 2022.
- [17] D. R. Morgan, Z. Ma, J. Kim, M. G. Zierdt, and J. Pastalan, “A Generalized Memory Polynomial Model for Digital Predistortion of RF Power Amplifiers,” *IEEE TRANSACTIONS ON SIGNAL PROCESSING*, vol. 54, 2006.
- [18] ebrary.net, “Generalized Memory Polynomial Model,” 2022.